Approaches to monitor ATP levels in living cells: where do we stand?

Seyta Ley-Ngardigal, Giulia Bertolin

Approaches to monitor ATP levels in living cells: where do we stand?

Seyta Ley-Ngardigal[1,2] and Giulia Bertolin[1,*]

[1] CNRS, Univ Rennes, IGDR (Genetics and Development Institute of Rennes), UMR 6290, F-35000 Rennes, France

[2] LVMH Research Perfumes and Cosmetics, 185 avenue de Verdun, F-45804 Saint Jean de Braye, France

[*] Correspondence: giulia.bertolin@univ-rennes1.fr; Tel: +330223237516

Running title: ATP production mechanisms and how to measure them.

Abbreviations: $\Delta\Psi$m, mitochondrial membrane potential; AAC, ADP/ATP carrier; ADP, Adenosine Diphosphate; AMP, Adenosine Monophosphate; ANT, Adenine Nucleotide Translocator; ARSeNL, ATP detection with a Ratiometric mScarlet-NanoLuc sensor; ATEAM, Adenosine 5'-Triphosphate indicator based on Epsilon subunit for Analytical Measurements; ATP, Adenosine Triphosphate; BRET, Bioluminescence Resonance Energy Transfer; CFP, Cyan Fluorescent Protein; CyPD, cyclophilin D; EAF-ATP, Enhanced Acceptor Fluorescence-based ATP biosensor; ECL, electrochemiluminescence; ESI, ElectroSpray Ionization; FAD, Flavin Adenine Dinucleotide coenzyme; FCCP, carbonylcyanide p-trifluoromethoxyphenylhydrazone; FMN, Flavin Mononucleotide coenzyme; FRET, Förster's Resonance Energy Transfer; GCE, Glassy Carbon Electrode; GFP, Green Fluorescent Protein; iATPSnFR, intensity-based ATP-sensing fluorescent reporter; HPLC, High-Performance Liquid Chromatography; LC-MS/MS, Liquid Chromatography coupled to tandem Mass Spectrometry; MALDI, Matrix Assisted Laser Desorption Ionization; MaLion, Monitoring aTP Level intensiometric turn-on indicator; MCF, Mitochondrial Carrier Family; MRS, Magnetic Resonance Spectroscopy; NAD, Nicotinamide Adenine Dinucleotide; NMR, Nuclear Magnetic Resonance; mPTP, mitochondrial Permeability Transition Pore; P_i, inorganic phosphate; PBA, Phenyl Boronic Acid; PiC, phosphate carrier; PolyP, inorganic polyphosphate; QD, Quantum Dots; QUEEN, Quantitative Evaluator of cellular Energy; R6G, Rhodamine 6G; ROS, Reactives Oxygen Species; SPG7, Spastic Paraplegia 7; VDAC, Voltage-Dependent Anion Channel; VNUT, Vesicular Nucleotide Transporter; YFP, Yellow Fluorescent Protein;

Keywords: ATP, ATP synthase, mitochondria, biochemical assays, fluorescence-based tools.

Conflicts of Interest : The authors declare no conflict of interest.

Abstract: ATP is the most universal and essential energy molecule in cells. This is due to its ability to store cellular energy in form of high energy phosphate bonds, which are extremely stable and readily usable by the cell. This energy is key for a variety of biological functions such as cell growth and division, metabolism, signaling, and for the turnover of biomolecules. Un-

derstanding how ATP is produced and hydrolyzed with a spatiotemporal resolution is necessary to understand its functions both in physiological and pathological contexts. In this review, we will first describe the organization of the electron transport chain and ATP synthase, the main molecular motor for ATP production in mitochondria. Second, we will review the biochemical assays currently available to estimate ATP quantities in cells, and we will compare their readouts, strengths and weaknesses. Finally, we will explore the palette of genetically-encoded biosensors designed for microscopy-based approaches, and show how their spatiotemporal resolution opened up the possibility to follow ATP levels in living cells.

1. Introduction: ATP production and functioning of the ATP synthase

ATP (or Adenosine Triphosphate) is a key and universal energy molecule with the ability to store and transport energy. This is achieved thanks to the phosphoanhydride bonds between the α – β phosphate groups, and between the β – γ ones. These are defined as high energy bonds, because their hydrolysis is energetically favorable in both intracellular and extracellular environments [1,2]. The term "high energy bond" to define phosphoanhydride bonds is a shortcut first appeared in literature in the 70s, because of the high free energy (G) of the ATP hydrolysis reaction. Indeed, this type of bonds does not have intrinsically high energy levels, but their rupture in a particular molecular environment such as the living cell releases a large amount of energy. The products formed after an ATP hydrolysis reaction have a lower free energy content, hence the term of "high energy bond" to describe phosphoanhydride bonds [3].

From a biological point of view, the energy released from the hydrolysis of the phosphoanhydride bonds is essential to almost all cellular processes and it is consumed to perform a various number of reactions as anabolism [4], ion transport [5], synaptic communication [6,7] and muscular contraction [8]. Overall, cellular activities can be seen as energy-consuming processes, where ATP is the most common energy source [2,9]. In addition to its energy-providing role, ATP is also a key molecule involved in cell signalling [10], and particularly in purinergic signaling [9]. In this context, ATP has the ability to be recognized by

purinergic receptors and plays key roles in inflammation [11,12], coagulation, cell proliferation, synaptic transmission and cell permeability among other roles [13–15].

From a structural point of view, there are significant electrostatic repulsions between the negatively-charged phosphate groups of the ATP molecule. As a result, ATP tends to undergo spontaneous hydrolysis. Because of this feature, ATP (as well as ADP, Adenosine Diphosphate) forms a complex with the magnesium ion (Mg^{2+}) within the cell. The Mg^{2+}-ATP complex reduces the electrostatic repulsions within the ATP molecule, due to the positive charge of the Mg^{2+} ion that partially neutralize the negative charge of oxygen. This makes the Mg^{2+}-ATP complex less prone to spontaneous hydrolysis, thus more stable in the cell than ATP in its free form [16] (Figure 1).

Due to its particular structure in terms of size and charge [17], the transport of ATP across the cell membrane and the intracellular membranes requires specific transporters [18,19]. Generally speaking, transporters are ATP/ADP carriers which allow the import of ATP and the export of ADP inside a particular compartment [20,21]. Transporters can be found at the level of mitochondria, the endoplasmic reticulum, of the Golgi apparatus, and of peroxisomes. Of note, the vesicular transport of ATP by the Vesicular Nucleotide Transporter or VNUT has also been described, acting mainly in the brain and in the adrenal gland [22]. The transport of ATP across mitochondrial membranes is essentially ensured by mitochondrial carriers (MCF). Three major classes of MCF have been described: the ADP/ATP carrier (AAC or Adenine Nucleotide Translocator, ANT), localised at the inner mitochondrial membrane and allowing the export of ATP by importing ADP [23–26]; the ATP-Mg/P_i carrier, which allows the exchange of ATP-Mg^{2+} for HPO_4^{2-} between the cytosol and the mitochondrial matrix [27,28]; the AMP/ATP carrier, found exclusively in plant mitochondria and allowing the export of ATP and the import of AMP [29].

The mechanisms of ATP transport are intimately linked with the membrane potential of the corresponding organelles or of the secreting vesicles. In mitochondria, the membrane

potential (ΔΨm) is not only essential for MCFs to orchestrate the translocation of nucleotides, but also for energy production, and for the quality control of mitochondria by mitophagy [30]. The mitochondrial membrane potential is maintained by the activity of the electron transport chain and the reverse activity of the ATP synthase, which will be described in the next sections. Interestingly, a non-correlation between ΔΨm and ATP production has been described to occur during axonal elongation processes [31]. Although ΔΨm is essential for the production of mitochondrial ATP, these recent data indicate that it should not be used as a direct readout of the quantity of ATP produced by the organelles.

Due to the multiple and pivotal roles of ATP, the eukaryotic cell established multiple pathways to synthesize this essential molecule. The energy-providing biomolecules are carbohydrates, lipids and proteins, and are mostly obtained with food intake. These molecules allow ATP to be synthesized by different catabolic pathways as glycolysis, lipolysis and proteolysis, respectively. Each of these pathways converges on a common pathway: oxidative phosphorylation, which is the main route for aerobic ATP synthesis [32]. In the sections below, we will focus on the comparison between the bacterial and eukaryotic complexes orchestrating oxidative phosphorylation, and on structural insights of the ATP synthase.

1.1 Oxidative phosphorylation

Oxidative phosphorylation is the process coupling the oxidation of electron-donor molecules –$NADH,H^+$ and $FADH_2$ – with the phosphorylation of ADP into ATP. This process takes place at the level of the inner mitochondrial membrane, within the mitochondrial respiratory chain. Functionally speaking, the mitochondrial respiratory chain can be divided into the electron transport chain module (complexes I to IV) and the ATP synthase (complex V) (Figure 2).

The electron transport chain is constituted of four large protein complexes (I, II, III and IV) as well as two membrane shuttles, coenzyme Q and cytochrome c (Figure 2) [33].

Complex I, also called NADH dehydrogenase, is a complex of approximately 1000 kDa and is composed of 45 protein subunits, 1 flavin mononucleotide coenzyme (FMN, similar to FAD) and 8 iron-sulfur clusters. It catalyzes the transfer of electrons from NADH,H^+ to coenzyme Q, while translocating protons across the inner mitochondrial membrane into the intermembrane space [34,35]. Complex II, also named succinate dehydrogenase, is a complex of approximately 140 kDa and is composed of 4 protein subunits, 1 flavin adenine dinucleotide coenzyme (FAD), 3 iron-sulfur clusters and 1 single heme group. It catalyzes the transfer of electrons from succinate to coenzyme Q10 [35]. Complex III, named cytochrome c reductase, is a complex of approximately 250 kDa and is composed of 11 subunits, 1 iron-sulfur cluster and 3 cytochromes (1 cytochrome c_1 and 2 cytochromes b). It catalyzes the transfer of electrons from coenzyme Q to cytochrome c, and it translocates protons across the inner mitochondrial membrane into the intermembrane space [35]. Complex IV, also named cytochrome c oxidase, is a complex of approximately 200 kDa and is composed of 13 subunits, 3 copper atoms and 2 heme groups, also known as cytochrome a and cytochrome a_3. It catalyzes the transfer of electrons from cytochrome c to oxygen, and it translocates protons across the inner mitochondrial membrane into the intermembrane space [35]. Last, the shuttles function as follows: coenzyme Q, also called CoQ or ubiquinone, is a liposoluble electron carrier and transports both electrons and protons [36], while cytochrome c is a water-soluble protein which carries electrons exclusively [37].

In mitochondria, the respiratory chain complexes were shown to assemble into supercomplexes called respirasomes [38], with the following composition: (complex I)$_1$-(complex III)$_2$-(complex IV)$_{1-2}$ or (complex III)$_2$-(complex IV)$_{1-2}$. In addition, the association of multiple respirasomes into a megacomplex, composed by (complex I)$_2$-(complex III)$_2$-(complex IV)$_2$ has been described. [38] (Figure 3). The association of the respiratory chain complexes in respirasomes or megacomplexes has many advantages [39]. First, complex I was shown to have an increased stability when it is integrated into a supercomplex. Second, respirasomes produce less reactives oxygen species (ROS) than individual complexes, since the ROS

formation sites are less accessible. Third, the catalytic activity of the complexes forming the respirasome was shown to be greater in terms of proton transfer and electron transport rates. In light of this feature of supercomplexes and unlike complex I, III and IV, complex II does not participate to the formation of supercomplexes. This is most likely due to its inability to transfer protons from the mitochondrial matrix to the intermitochondrial space. [39–41]. Last, the link between the ultrastructural characteristics of mitochondria and their overall number appears to be tissue-specific, and optimized to better respond to *in-situ* energy demands [42,43]. Similarly, the quantity and the distribution of supercomplexes and megacomplexes inside mitochondria were shown to dynamicall adapt to the type of tissue, as well as to physiological and metabolic conditions [44–50].

In summary, the role of these first four complexes is to oxidize electron-donor molecules such as $NADH,H^+$ and $FADH_2$, which are derived from the Krebs cycle, and which are powered by the catabolism of carbohydrates, lipids and proteins. The electrons are then transferred to O_2, thereby making this process aerobic. This successive oxidation of donor molecules creates a proton gradient, allowing the phosphorylation of an ADP molecule into ATP by the ATP synthase complex. The ATP synthase (complex V) can also arrange in supramolecular complexes as dimers and tetramers (Figure 3). The clustering of multiple ATP synthase complexes triggers local folding events on the inner mitochondrial membrane, commonly known as mitochondrial *cristae* [53,54]. We will deepen the description of this ATP factory in the next paragraph [9].

1.2 ATP synthase

The process of ATP synthesis by oxidative phosphorylation is a phenomenon already existing in bacteria, that have a membrane respiratory chain very similar to the mitochondrial one (Figure 2). This similarity between the bacterial and mitochondrial respiratory chains became one of the pillars of the theory of primary endosymbiosis, which explains the origin of mitochondria in eukaryotic cells as the result of the endocytosis of bacteria by a primitive

eukaryotic cell [55–57]. It is thought that during evolution, this primitive eukaryotic cell maintained an endosymbiontic relationship with bacteria, which then transformed into mitochondria approximately between 1.5 to 2 billion years ago [58]. In support of this theory, the main "energy currency" unit of bacterial cells is inorganic polyphosphate (polyP). PolyP is a polymer of few to several hundred phosphate molecules linked by phosphoanhydride bonds, similarly to ATP (Figure 1) [59]. This molecule provides energy and phosphate storage, and it contributes to the conversion of AMP into ADP, and from ADP into ATP [60,61]. PolyP is also found in mammalian cells, and its production is directly linked to mitochondrial respiration in the activation and/or formation of the mitochondrial Permeability Transition Pore described below [59,62,63]. Although the endosymbiontic theory is becoming increasingly controversial [64–66], the first analyses of the ATP synthase were carried out on the bacterial one due to its similarity with the human cognate complex, the fast replication rates of bacteria, and the ease of introducing modifications to the bacterial genome [67].

ATP synthase is a large complex of about 600 kDa and it consists of three parts: the F0 unit, the F1 unit and the peripheral stalk. The F0 unit is embedded in the inner mitochondrial membrane (or the bacterial plasma membrane), and it is responsible for proton translocation (Figure 4). This unit rotates within the membrane upon its interaction with protons, hence its nickname "rotor". F0 also forms a central stalk, which connects it to the F1 unit. The F1 unit protrudes in the mitochondrial matrix (or the bacterial cytoplasm), and is the static unit of the ATP synthase or "stator". From a functional point of view, F1 is responsible for the phosphorylation of ADP into ATP. In addition to a direct connection between F0 and F1 by the central stalk, the two unit are also connected by a peripheral stalk. The peripheral stalk further stabilizes the complex, and allows to keep the entire ATP synthase complex stable and static during the rotation of the c-ring and within the hexamere α_3-β_3 [68] (Figure 4, 5).

From a structural point of view, the bacterial and mitochondrial ATP synthases show high similarities in their F0, F1 and peripheral stalk units. The bacterial F0 unit is composed of subunits a-$c_{9\text{-}15}$, the F1 unit is composed of subunits α_3-β_3-γ-ε and the peripheral stalk is

composed of subunits b_2-δ [67]. Similarly, the mitochondrial F0 unit is composed of subunits a-$c_{8\text{-}15}$, the F1 unit is composed of subunits α_3-β_3-γ-δ-ε and the peripheral stalk is composed of subunits OSCP-b_2-d-F6. In addition to the differences observable between the two peripheral stalks, the mitochondrial ATP synthase is composed of some additional subunits – e, g, f, A6L, j and k – which are associated to the F0 part [69,70] (Figure 4).

Being structurally very similar, the bacterial and mitochondrial ATP synthases synthesize ATP on the same principle, the rotational catalysis (Figure 5). As introduced above, the electron transport chain causes an efflux of protons towards the mitochondrial intermembrane space (or bacterial periplasmic space), thereby creating a proton gradient. Through the F0 unit of ATP synthase, the flux of protons is then re-internalized from the mitochondrial intermembrane space (or bacterial periplasmic space) to the mitochondrial matrix (or bacterial cytoplasm). Mechanistically, the proton flux induces the rotation of the rotor part, thanks to the interactions between protons and aspartate residues on the c subunits of the F0 unit. The rotation of F0, including the central stalk which is in the core of the F1 unit, results in conformational changes of the α_3-β_3 hexamer. The nucleotide-binding sites are located at the interface of α and β subunits. It is at the level of the β subunits that ATP is directly synthesized, thanks to the presence of a catalytic site within each subunit. The α subunits do not play an active role in catalysis, but they participate to the regulation of the ATP synthase activity [70]. Each of the β subunits has a given conformation (Figure 5): the first is the loose conformation, also called β_{DP} because it binds ADP and inorganic phosphate (P_i); the second is the tight conformation or β_{TP}, because it forms a bond between ADP and P_i and synthesizes ATP. The last is the open conformation, also called β_E or empty, because it releases the newly-formed ATP molecule. These different conformations work in synergy to synthesize or hydrolyze ATP and at each timepoint, each of the β subunits is occupied by a nucleotide [71]. Of note, a recent study reported that the β subunit does not undergo successive rotations of 120°, but a series of rotations of 80° + 40° [72]. This would lead to six distinct conformations, and not only three as documented so far.

Dimers of ATP synthase have the capacity to form a mitochondrial Permeability Transition Pore (mPTP), also known as mitochondrial megachannel (MMC) [73,74] (Figure 6). The OSCP and c subunits of ATP synthase are the main proteins involved in this structure. The OSCP subunit, in association with cyclophilin D (CyPD) leads to the opening of the mPTP, while the c-subunit forms a voltage-sensitive channel leading to cytosolic calcium overload [75–77]. Although the composition of the mPTP is becoming increasingly clear, the exact protein associations within this structure are still under intense investigation [78,79]. Beyond its association with CyPD, recent studies highlighted that mPTP can associate with mitochondrial proteins such as ANT, the outer membrane voltage-dependent anion channel (VDAC), the phosphate carrier (PiC) and paraplegin matrix AAA peptidase subunit (SPG-7 or spastic paraplegia 7) (Figure 6) [80–82]. The ATP synthase / PiC / ANT complexes were also shown to assemble into the so-called "Mitochondrial ATP synthasome", a structure coordinating the entry of Pi and ADP into mitochondria with the synthesis of ATP via ATP synthase [83–85].

The mechanisms leading to the opeining or closing of the PTP are well described [78]. Among the factors stimulating the opening of the PTP, there are elevated concentrations of calcium or elevated concentrations of reactive oxygen species (ROS), free fatty acids, the reduction of transmembrane potential and the binding of CyPD on the OSCP subunit of ATP synthase [78,86–88]. Among the factors inhibiting the opening of the mPTP, there are alterations in nucleotides or magnesium concentrations, coenzyme Q10 and binding of cyclosporine A (CsA) on CyPD [78,89,90]. Brief and reversible openings of the mPTP were shown to participate to calcium homeostasis within mitochondria, and they allow the bidirectional passage of small molecules of less than 0,3 kDa. However, when the opening of the mPTP is long, it becomes irreversible and causes the bidirectional passage of molecules up to 1,5 kDa. As a consequence, mitochondria become waterlogged and swell, lose their internal architecture and release pro-apoptotic factors leading to cell death by apoptosis and necroptosis [78,79,91]. This mechanism can also be used by tumor cells to increase their resistance to cell death by desensitizing the mPTP to calcium and ROS. In this light, the mPTP became a prominent target for anticancer strategies [92].

To summarize, the entire electron transport chain and ATP synthase therefore form a powerful and efficient combination for ATP production, both in bacteria and in eukaryotic cells. Given that the intracellular functions of ATP are critical for cell physiology and in pathological conditions, monitoring ATP levels in cells has been used for decades as readout of cellular functionality. First analyzed using biophysical and biochemical approaches, the raise in microscopy-based techniques has deepened our understanding of the many roles of ATP in the cell.

In the section below, we will first describe the most employed biochemical and biophysical assays to monitor ATP levels in quantitative or qualitative way. Second, we will review the panel of microscopy-based tools and approaches to monitor cellular and extracellular ATP levels at the single-cell level and with spatiotemporal resolution.

2. Biochemical and biophysical approaches to measure cellular and extracellular ATP levels

2.1. Nuclear Magnetic Resonance spectroscopy

Nuclear Magnetic Resonance (NMR) is a technique based on the property of specific atoms to have an odd number of protons and/or neutrons. This results in a non-zero nuclear spin (*I*). Atoms as ^{1}H, ^{13}C, ^{19}F and ^{31}P, have an *I* value equal to ½, making them comparable to magnetic dipoles. When these atoms are subjected to a magnetic field, they absorb an electromagnetic wave and resonate by emitting an energy peak detectable with a NMR spectrometer [93]. Since ATP, ADP and AMP (Adenosine Monophosphate) molecules contain a significant proportion of H and P atoms, they behave as magnetic dipoles and it is possible to detect them using this approach [94–96] (Figure 7).

The quantitative Nuclear Magnetic Resonance spectroscopy (qNMR) is a variant of NMR allowing, as the name indicates, to quantitatively measure one or more molecules simultaneously [97]. On a qNMR spectrum, the peak area is directly proportional to the number of atoms. The concentration of the molecules analyzed can be determined by using an internal standard (as TMSP or Na_2HPO_4) of known concentration previously added to the sample. By using ^{1}H and ^{31}P qNMR (^{1}H-NMR and ^{31}P-NMR), Lian et al. were able to simultaneously monitor ATP, ADP and AMP [96]. The main advantage of this method is the perfect linearity in a given range: 0.1–100 mM for ^{1}H-NMR, and 1–75 mM for ^{31}P-NMR. qNMR turned out to be particularly useful in pathological situations where cytoplasmic ATP is massively released into the circulation [98]. However, this technique has some limitations: first, the detection range is lower than the concentration of physiological ATP present in cells and tissues. Furthermore, this technique has a low temporal resolution, as it requires an extended time frame – approximately of 14 hours – to complete the detection of a specific spectrum. In addition, and although extremely precise in estimating the quantity of specific components, qNMR requires significant amounts of biological materials (e.g. total cell extracts) to provide reliable readouts on the concentration of nucleotides in physiological conditions.

Last, NMR requires very expensive equipments that prevent its thorough diffusion in every lab interested in analysing ATP levels.

2.2. High-Performance Liquid Chromatography and Liquid Chromatography coupled to tandem Mass Spectrometry

High-Performance Liquid Chromatography (HPLC) is a widespread technique, which has been widely used since the 1990s. Its purpose is to separate molecules within a complex sample according to specific features such as polarity [102]. This method is based on a mobile phase, which is constituted by the sample to analyse, previously resuspended in a solvent with a given polarity. The mobile phase then passes through a column, which constitutes the stationary phase. The molecules in the sample will be separated thanks to their different affinities with the column: those with more affinity will be retained on the stationary phase, while the others will be washed out. As a result, the molecules will be separated and will exit the column at different times. At the exit of the stationary phase, the molecules will pass through a detector for analysis, thus generating a chromatogram (Figure 8). Globally, this approach allows to identify the nature of the molecules analysed and their absolute quantity [102].

HPLC has thoroughly been used to determine ATP, ADP and AMP levels in different types of samples, like in plant primary cells [103], in conventional mammalian cell lines such as MCF7 and MDA436 [104], or in primary cells such as human and mouse platelets [105]. The sensitivity of HPLC in detecting nucleotides is in the order of µmol, therefore HPLC analyses on biological samples require large amounts of cells and a complete extraction of cell contents. This is a potential caveat, as complete extractions can lead to the loss of nucleotides due to hydrolysis. To counteract this limitation, Bhatt et al. have developed an ion-pairing HPLC method coupled with fluorescence detection to quantify ATP, ADP and AMP in primary

astrocytes [106]. In ion-pairing HPLC, the stationary phase consists of an ion-pairing column, and an ion pair reagent is added to the mobile phase to increase or decrease the retention time of partly-ionized organic analytes in the column, according to the type of molecule to analyse. In addition, the method to detect nucleotides at the exit of the column benefits from the sensitivity of fluorescence (nmol/pmol range). Nucleotides undergo a derivatization by the transformation of adenine-based nucleotides into 1,N^6-etheno derivatives, which gives them fluorescent-like properties and protects them from hydrolysis during cell extraction. This method relies on an excitation wavelength at 280nm and on a emission wavelength at 410nm, specific for etheno-adenine compounds. Unlike conventional HPLC, ion-pairing HPLC is extremely precise and capable to monitor the levels of nucleotides at the pmol scale. However, it still requires complete cell extraction and a modification step to make ATP, ADP and AMP fluorescent. Compared to NMR, HPLC is a fast (the retention time is about 20 min [106]), automated, highly reproducible and very accurate method to identify nucleotides in total cellular extracts. As for NMR, this technique is very expensive, thereby hindering its diffusion as a gold-standard method to quantify nucleotides in living samples.

The Liquid Chromatography coupled to tandem Mass Spectrometry (LC-MS/MS) combines the ability to separate different molecules by liquid chromatography as in HPLC, and the ability to detect and identify molecules of interest by measuring their mass using mass spectrometry. Briefly, mass spectrometry is based on the ionization of molecules of interest (generally by ElectroSpray Ionization, ESI; or Matrix Assisted Laser Desorption Ionization, MALDI) and their sublimation [107]. Once ionized, the molecules enter an acceleration zone in which they acquire a specific speed, which directly depends on their mass (m) and charge (z). Then, the molecules are sorted according to their m/z ratios in an analyzer, which is constituted by an empty column of air preserving the respective speed of each molecule against friction forces. Once the molecules have gone through the analyzer, an ion detector detects the molecules individually and generates a spectrum (Figure 9).

The LC-MS/MS method benefits from the advantages of LC to separate molecules according to their polarity, while MS/MS allows to determine their quantity with high precision. Recent studies used LC-MS/MS for the simultaneous quantification of ATP and other small metabolites as 2,3-diphosphoglycerate, NAD^+/$NADH,H^+$ or short chain acyl-CoAs [108,109]. Therefore, this method makes it possible to obtain the concentration of ATP and that of other molecules with very different biochemical properties, at the same time and faster than the previous approaches (retention time is between 2 min [109] and 10 min [108], according to the setup used). However like HPLC, LC-MS/MS requires expensive instruments and sample preparation can be cumbersome.

2.3. Respirometry

Respirometry (or oxygraphy) is an indirect, qualitative-only method to measure the efficiency of mitochondrial ATP production, although it is a convenient and less expensive technique than NMR and HPLC to measure ATP levels.

As described above, the electron transport chain creates a proton gradient by consuming oxygen, which in turn allows the ATP synthase to rotate and produce ATP from ADP+P_i (Figure 2). Oxygen consumption can directly be linked to ATP production: the more cells produce ATP, the more oxygen they consume [110]. The principle of oxygraphy is to modulate the respiratory chain using selective drugs and metabolites known for their capacity to activate or inhibit its activity, and to measure the corresponding flux of oxygen. The most common technologies to perform respirometry are the high-resolution Oxygraph-2k (O2k, Oroboros Instruments, Austria), and the sensitive, high-throughput Seahorse XF Extracellular Flux Analyzer (Seahorse XF, Seahorse Bioscience Inc.). These setups were shown to perform efficiently on isolated mitochondria, cultured cells, and tissues [111–113], and their output is complementary [111]. Overall, the sample is placed in a specific support before undergoing the sequential injection of different drugs and / or metabolites. The cocktail of drugs used in an oxygraphy experiment classically contains oligomycin, FCCP (carbonylcyanide p-

trifluoromethoxyphenylhydrazone) and a mix of antimycin-rotenone, while succinate, ADP and cytochrome c are the most commonly-used metabolites (Figure 10).

Oligomycin is an antibiotic which inhibits the ATP synthase by associating with the F0 subunit, and prevents the backflow of protons to the mitochondrial matrix [114]. This results in low or no oxygen consumption, and thus no ATP production. FCCP is a weak and lipophilic acid which acts as an ionophore and a uncoupling agent. Its lipophilic properties allow FCCP protonation in the intermembrane space. Then, FCCP freely crosses the inner mitochondrial membrane and returns to the mitochondrial matrix. Once there, it deprotonates itself before re-crossing freely the inner mitochondrial membrane and being re-protonated in the intermembrane space. Because of these protonation/deprotonation cycles on the FCCP molecule, the protons bypass the ATP synthase almost completely. Oxygen consumption is therefore maximized, but there is almost no ATP synthesis by the ATP synthase [115]. Last, antimycin is an antibiotic blocking the electron transfer at complex III [116]. It is often used in combination with rotenone, an insecticide blocking electron transfer at complex I [117]. The antimycin/rotenone mix blocks the overall electron transfer of the respiratory chain and as a consequence, the electrons can not be transferred to oxygen. As a result, the proton gradient no longer exists, and ATP synthesis by the ATP synthase stops (Figure 10).

In conclusion, NMR, HPLC and LC-MS/MS allow the direct quantification of global ATP levels from cell extracts and serum samples previously denaturated. Recently-developed techniques such as phosphorous-31 (31^P)-Magnetic Resonance Spectroscopy (31^P MRS) and magnetic resonance imaging (MRI) allow for ATP quantifications in complex biological samples and *in vivo*, although the acquisition time to complete one reaction remains excessively long, and the spatial resolution poor [118,119]. Conversely, oxygraphy allows to work on intact samples without prior denaturation, but the measurement of ATP production is inferred from oxygen levels, and remains therefore indirect. Overall, these are widely-employed, robust and reproducible methods. However, these approaches are hardly compatible with real-time

analyses, and do not provide a sufficient spatiotemporal resolution. Indeed, phosphorylation of ADP to ATP occurs in seconds, while any analysis performed with the methods described above occurs in minutes or hours [120]. This is the reason why the development of tools based on microscopy represented a significant advance in the field. As described below, these tools allow to detect different pools of ATP (i.e. organellar, cellular and extracellular) with high spatiotemporal resolution, and they improved our understanding of the mechanisms of ATP production at the single-cell level.

3. Microscopy-based tools approaches to measure cellular and extracellular ATP levels

In the last years, huge efforts have been made to develop tools capable of detecting ATP levels in living cells, but also at the subcellular level and with sufficient spatiotemporal resolution.

In the sections below, we will explore the probes using electroluminescence, chemiluminescence and bioluminescence to estimate ATP levels, with a particular focus on fluorescence-based biosensors. Fluorescence-based biosensors are built on three selective properties of fluorophores: 1- the quantum yield of each fluorophore, that is the ratio between the number of photons emitted and the number of photons absorbed; 2- specific excitation and emission wavelengths (λ) that allow to use probes individually or in combination; 3- the specific lifetime of their excited state, that is the time between the excitation of a molecule of fluorophore and its return to the fundamental state [121,122] (Figure 11).

3.1. Electrochemiluminescence-based tools

The electrochemiluminescence (ECL) is a technique which is initiated by a step of electron transfer to the surface of an electrode. Several studies used this highly-performing and sensitive technique to detect and quantify ATP [123–125]. Liu et al. developed an ECL ATP sensor which turns on or off when ATP is bound or unbound, respectively [123] (Figure 12). This method is based on the use of Quantum dots (QDs), aptamers and DNAzyme. QDs, also called "artificial atoms", are semiconductor nanostructures capable of collecting electrical charges and emitting light according to their size. The QDs are attached to an electrode (Glassy Carbon Electrode, GCE), and then linked to a DNA sequence (hereby called DNA1). The DNA1 is partially complementary with the aptamer, a synthetic oligonucleotide capable of binding a specific ligand such as ATP. The DNA1 allows the aptamer to be linked to the QDs. The complex "QDs - DNA1 - Aptamer" forms an aptasensor, and it will synergistically work with the signal

probe called DNAzyme, an oligonucleotide capable of performing a specific chemical reaction. Here, the DNAzyme is carried by a gold nanoparticle and consists of a second DNA sequence (hereby called DNA2), which is also partially complementary to the aptamer and associated with a hemin molecule, a porphyrin playing the role of an electron-binding cofactor. This DNA2-hemin association then forms a secondary structure called G-quadruplex, and it constitutes the signal probe. If there is no ATP, the aptasensor is linked to the signal probe, which is able to reduce oxygen to hydroxide anion and induces a drastic decrease in the ECL emission. Conversely, the aptamer preferentially binds to the ATP molecule when it is present. As a result, the aptamer and the signal probe detach from the QD-modified electrode, allowing a significant ECL emission (λem=610nm).

This method of detecting ATP was originally validated on human serum samples, as first-generation QDs necessitated a liquid medium for better results. Recently, the use of QDs has become more diffused and although their use in medicine is still largely unexplored, *in vivo* analyses using mouse models seems promising [126,127]. This ECL-based technique seems to be very sensitive to detect ATP levels (detection at nanomolar scale), and the use of quantum dots for live cell imaging is more and more widespread [128]. However, this technique should be further optimized to use it in single-cell imaging applications, and to obtain a better spatiotemporal resolution in living samples.

3.2. Chemoluminescent-based tools

Chemoluminescent-based tools or chemosensors are based on the chemical properties of ATP itself, which is capable of carrying out interactions of different nature (covalent, electrostatic, hydrogen bonds, etc…) with its substrates. This is due to the chemical structure of ATP, containing three negatively charged phosphate groups, an aromatic adenosine and a molecule of ribose with several hydroxyl groups. The vast majority of chemosensors are single-

wavelength ratiometric sensors, therefore requiring a spectrometer to quantify the presence of ATP [122].

The most significant chemosensors are based on rhodamine, a small organic molecule which emits fluorescence due to its xanthene nucleus (λ_{em}=558nm). The rhodamine-based probe called Rh6G-NH-PBA consists of rhodamine 6G (Rh6G), a diethylenetriamine group (NH) and a phenyl boronic acid group (PBA) (Figure 13). In the absence of ATP, the probe does not emit light thanks to its closed ring structure. Conversely, three specific interactions will take place in the presence of ATP: 1- covalent interactions between PBA and the ribose molecule of ATP; 2- π-π interactions between the xanthene nucleus of Rh6G and the adenine of ATP; 3- electrostatic interactions between the amino groups of NH and the phosphate group from ATP [129]. These interactions trigger the opening of the ring and free the light-emiting properties of Rh6G, which can then be detected.

The use of small organic molecules as Rh6G allows to obtain an excellent selectivity for ATP over ADP and AMP, but also to monitor mitochondrial ATP fluctuations in live cells [122]. However, some biophysical properties of this probe still remain to be elucidated. It has been previously shown that rhodamine B, which is a lipophilic cation, accumulates in the mitochondrial matrix [130], and it has been suggested that this accumulation may result from a combination of the negative mitochondrial membrane potential, the high viscosity of the organelle, and ATP concentration in mitochondria [131]. Although rhodamine-based probe turned out to be a real advance in monitoring of mitochondrial functions and in particular to determine ATP levels [132,133], they also show very important limitations for live cell imaging, as aggregation, quenching and low photosensitivity [134].

3.3. Genetically-encoded ATP biosensors

We will now explore biosensors based on specific fluorescent properties such as FRET (Förster's Resonance Energy Transfer), BRET (Bioluminescence Resonance Energy Transfer) and intensiometric / ratiometric single-fluorophore probes. In general, these tools rely on the conformational changes of a bacterial protein, the *Bacillus subtilis* ATP synthase subunit ε (Figure 14). This subunit corresponds to the mitochondrial ATP synthase subunit δ (Figure 4), and it has been thoroughly used because of its many advantages. First, it is capable of binding ATP without hydrolyzing it [135–137]. Furthermore, the ε subunit can bind ATP with higher specificity than ADP, GTP, UTP, and CTP [136]. Then, it undergoes detectable conformational changes when binding to ATP (Figure 14) [138,139]. Using proteins of bacterial origin to engineer sensors is a commonly-used approach [140], as it potentially avoids the establishment of non-specific interactions with endogenous mammalian proteins. In the case of the ε subunit, a mutated version with humanized codons has been used in sensors instead of its normal counterpart, and this to disrupt a hydrophobic patch required for the interaction with the γ-subunit of the endogenous mitochondrial ATP synthase [138]. In light of these considerations and improvements, the use of the *Bacillus subtilis* ε subunit of the ATP synthase seems to be a good strategy to study intracellular ATP fluctuations.

3.3.1. FRET-based biosensors to measure cellular and extracellular ATP levels

FRET microscopy relies on the transfer of energy between a donor/acceptor fluorescent pair. The energy transfer occurs only if the donor and acceptor are less than 10 nm apart and that the emission spectrum of the donor fluorophore overlaps the excitation spectrum of the acceptor fluorophore [143]. This technique is often used to study the physical interaction between two different proteins, and protein oligomerization (intermolecular FRET), or conformational changes of a given protein (intramolecular FRET); as for BRET-based probes, intramolecular FRET can be used to develop biosensors (Figure 15).

A large panel of fluorescent FRET-based ATP biosensors has already been developed. Nowadays, the most diffused probes to monitor ATP in single cells are the ATEAM biosensors (Adenosine 5'-Triphosphate indicator based on Epsilon subunit for Analytical Measurements). Originally developed by Imamura et al, the ATEAM biosensor comprises the ε subunit of the bacterial ATP synthase within a cyan (mseCFP, λex/λem=435/475 nm) and yellow (cp173-mVenus, λex/λem=515/527 nm) donor/acceptor pair at the N- and C-termini, respectively [138]. This biosensor allows the monitoring of intracellular ATP in living HeLa cells with subcellular resolution: ATP was detected in the cytoplasm, nucleus and the mitochondria by adding an organelle-specific localization signal to the biosensor. Taking advantage of organelle-specific variants of ATEAM, steady-state ATP levels in mitochondria of HeLa cells turned out to be lower than those detected in the cytoplasm or in the nucleus [138]. This suggests that either ATP synthesis by the ATP synthase is low, and/or ATP/ADP exchange rates are rapid in this model. Human skin fibroblasts expressing a mitochondrially-targeted ATEAM showed non-uniform fluorescence ratio signals [144], illustrating the differential capability of organelles to produce energy within the same mitochondrial network. In this model, the biosensor also uncovered the contribution of glycolysis to the maintenance of mitochondrial ATP levels [144]. More recently, the ATEAM probe has been used to compare ATP levels in the cytosol, at mitochondria and at the ER under metabolic stress. By using the 535/480 fluorescence ratio, the amount of ATP was reported to be higher in the cytosol (ratio ~ 3) than at mitochondria (ratio ~ 2.3), or at the ER (ratio ~ 1.5) [145]. Interestingly, it has been reported that ATEAM can undergo glycosylation events in other cellular compartments like the ER and Golgi, and that this post-translational modification makes it uncapable of detecting ATP at these locations [144,146]. However, there is no consensus in the literature on this point, and ATEAM appeared to report on ER ATP levels in an unperturbed manner in subsequent studies [147,148].

Unfortunately, the sensitivity of the donor/acceptor pair to the acidic pH of the lysosomes prevents its use and the estimation of ATP production at this compartment [144]. In a second version of the ATEAM biosensor, called GO-ATEAM, the original donor and

acceptor fluorophores were replaced by a green (cp173-mEGFP, λex/λem = 470/510 nm) and orange (mKOκ, λex/λem = 551/560 nm) fluorescent pair. This pair allows to have a more stable signal under acidic pH conditions, and a less phototoxic excitation wavelength than the one used to excite CFP in case of prolonged observations [149,150].

Further rounds of optimization of the ATEAM biosensor resulted in ATEAM1.03NL, where the introduction of mutations in the N-term and C-term domains of the ε subunit allows the monitoring of intracellular ATP levels at 25°C. This allowed the use of the ATEAM biosensor in *in vivo/ex vivo* models as *Drosophila melanogaster* and *Caenorhabditis elegans* [141].

By modifying the donor/acceptor pair, a EAF-ATP biosensor (Enhanced Acceptor Fluorescence-based ATP biosensor) was engineered. It consists of the ε subunit of bacterial ATP synthase as in the ATEAM biosensors, where the C-term and N-term domains are grafted with green (GFP, λex/λem = 488/507 nm) and yellow (YFP, λex/λem = 513/527 nm) fluorescent proteins, respectively. These fluorophores can be excited at similar wavelengths, which allows the emission of an enhanced fluorescence signal. This biosensor was used to monitor cytoplasmic ATP levels in cells lines derived from glioblastoma to better understand the metabolic switch from mitochondrial oxidative phosphorylation to cytoplasmic glycolysis – the Warburg effect – in this model [151].

Last, a re-engineering of the ATEAM biosensor was recently carried out to monitor extracellular ATP. The ecATEAM3.10 biosensor was expressed on the cell surface thanks to a PDGFR transmembrane anchor, with a CFP/YFP donor/acceptor FRET pair (CFP, λex/λem = 456/480 nm; YFP, λex/λem = 513/527 nm) [147]. As introduced above, ATP is also a key signalling molecule of purinergic signalisation, and this biosensor represents a useful tool to better understand the dynamics of this nucleotide as a messenger in the context of synaptic communication.

3.3.2. Bioluminescence and BRET-based tools to measure cellular and extracellular ATP levels

In bioluminescence, the emitted light is produced by an enzymatic reaction triggered by a luciferase. In the presence of O_2, ATP and Mg^{2+}, luciferase oxidises luciferin, its substrate, into oxyluciferin (Figure 16). This oxidation causes the emission of photons, and the resulting emission spectra is generally comprised between 546nm and 618nm according to the type of luciferase used [152]. Therefore, the capacity of luciferin to emit light is linked to the available amount of ATP in the surrounding environment. Light emission can thus be used to determine the concentration of ATP in plasma, mitochondria isolates or tissue extracts (global extraction of nucleotides can be performed by using perchloric acid) [153,154]. By adding a localisation signal to the luciferase, it is also possible to target cell subcompartments (mitochondria, cell membrane, nucleus, etc.) [146].

Rangajaraju et al. have developed a luciferase-based enzymatic system capable to monitor presynaptic ATP concentrations [155]. This luciferase-based tool is called Syn-ATP, and it consists of synaptophysin, a major synaptic vesicle protein, fused with luciferase and mCherry. The use of synaptophysin allows the targeting of the probe to nerve terminals, and the use of mCherry helps to determine the total amount of luciferase by performing a luminescence / fluorescence ratio. The Syn-ATP biosensor is a useful tool for researchers interested in exploring synaptic functions: the more ATP is consumed, the more bioluminescence levels – and therefore synaptic activity – are significant.

These types of solutions for ATP quantification are widely used and commercialised by several companies. However, this method has some notable caveats. First, certain luciferases have the capacity to produce ATP from the pool of ADP present in the sample, thereby showing poor specificity for the ATP produced after the oxidation of luciferin [156]. In addition, the enzymatic activity of luciferases can be perturbed by cellular inhibitors and by other cellular activities, which may reduce their capacity to perform bioluminescence [157].

To overcome these problems, the bioluminescence property of luciferase-like enzymes is used to develop biosensors based on the BRET phenomenon. BRET is based on the energy transfer between a bioluminescent molecule to a fluorophore. In the case where the luciferase and the fluorophore are close – less than 10 nm apart – the energy derived from a luciferase reaction excites the fluorophore [158]. BRET can be used to study the interactions between two different proteins or protein oligomerization (intermolecular BRET), or the conformational changes of a protein (intramolecular BRET). In this light, BRET-based biosensors rely on intramolecular BRET to monitor ATP (Figure 16). In such probes, the chosen luciferase generally does not require the consumption of endogenous ATP to oxidize luciferin into oxyluciferin (Figure 17), and this not to perturb endogenous signaling pathways.

Yoshida et al developed a BRET version of the ATEAM biosensor (a FRET-based biosensor described earlier) called BTEAM. This probe consists in the ATP binding domain of the ε subunit of bacterial ATP synthase flanked by Venus (yellow fluorescent protein, λem = 528 nm) at the N-ter, and a NanoLuciferase at the C-ter, which is an enzyme not relying on endogenous ATP to catalyse its reaction. This biosensor was shown to detect intracellular ATP in the cytoplasm (Cyt-BTEAM) or in the mitochondrial matrix (Mit-BTEAM) in live HeLa cells [159].

Following an analogous approach, Saito et al developed another variant of the ATEAM biosensor, called the Nano-lantern ATP biosensor. This sensor combines BRET and Complementation of Split Luciferase (CSL) [160], and it is built by placing Venus at the N-term of the sensor, while the ε subunit of the bacterial ATP synthase is inserted within two portions of the NanoLuciferase. When a molecule of ATP binds to the sensor, it allows the reconstitution of a full luciferase, and a BRET reaction between Venus and the Nanoluciferase can occur. This biosensor was validated on plant leaves to study ATP dynamics in the cytoplasm and in chloroplasts.

A third BRET-based ATP biosensor designed by Min et al, called ARSeNL (ATP detection with a Ratiometric mScarlet-NanoLuc sensor) consists of the ε subunit of the bacterial ATP synthase inserted between an mScarlet (red fluorescent protein, λem=594 nm) and a NanoLuciferase

[161]. This biosensor was shown to detect ATP levels in a HEK293A cell line and in mice. The major advantage of this biosensor is that it provides a stable and robust signal within animal tissues, and it seems to be particularly useful to study ATP levels in tumours [162].

BRET-based biosensors present many advantages. First, light emission comes from the enzymatic reaction triggered by the addition of the luciferase substrate, which eliminates the need for an external exciting light source (laser). This avoids the generation of autofluorescence and phototoxicity, two phenomena potentially harmful for live cells [163]. Moreover, BRET is extremely sensitive because this phenomenon occurs only when luciferase and the fluorophore are close [158]. For measurements on steady-states levels of ATP, this technique can be very useful and easy to perform, especially since luciferin is capable to cross the cellular membrane almost instantaneously, and it is not harmful to cell physiology [146,164].

However, BRET also shows an intrinsic limitation due to the luciferin itself. Indeed, some drug excipients such as cyclodextrin were shown to reduce bioluminescence levels inside cells [165]. This is a potential issue for studies focusing on drug development, since luciferin might interfere with the substance tested. For all these reasons, the creation of new luciferin variants, luciferases and acceptor fluorophores is a field under intense investigation [166,167]. In addition, the number of cells, the concentration of enzymes and of substrates can severely limit the quantification of BRET efficiency. As the light emitted is directly proportional to the amount of ATP in the cell, it is necessary to precisely quantify the initial number of cells. It is also necessary to ensure that the transfection of luciferase for BRET-based biosensors is homogeneous in cells, as the higher the concentration of the biosensor, the higher the amount of the emitted light. Finally, the amount of substrate to integrate into the medium to achieve a maximal detection of ATP must be carefully optimized.

3.3.3. Single-fluorophore ratiometric and intensiometric biosensors

Another class of biosensors is based on single fluorescent proteins, which exhibit a fluorescence signal or an increase in fluorescence emission at their corresponding wavelengths. This increase occurs only when the molecule of interest, in this case ATP, binds to the sensor and changes its conformation (Figure 18). In these probes, the most common fluorophores are circularly-permutated fluorescent proteins. Indeed, circularly-permutated fluorophores have their N- and C-termini directly fused with a peptide linker, thereby creating new terminal ends close to the chromophore. As a result, the slightest change in conformation is easily detected by the chromophore, which changes its fluorescence properties [168]. Within this class of probes, the QUEEN biosensor (Quantitative Evaluator of cellular ENergy) is a genetically-encoded, ratiometric fluorescent ATP indicator that allows to quantify global ATP levels inside bacteria and yeast [169]. This biosensor consists of a single circularly-permutated enhanced GFP (λex/λem = 400-494/513 nm) inserted between 2 α-helices of the ε subunit of the bacterial ATP synthase. The integration of circularly-permutated enhanced GFP into a flexible region of a sensory domain, as the ε subunit, allows to sense slight changes in its conformation. When ATP binds to the biosensor, we observe a shift of the 400/494 nm ratio, which is proportional to the concentration of ATP. Yaginuma et al [169] compared the capacity of the QUEEN biosensor to report on ATP concentration levels with classical luciferase ATP assays in bacterial cells. They showed that the results obtained with the QUEEN biosensor are almost equal to those obtained from bioluminescence luciferase assays.

Second, another ATP biosensor based on fluorescence intensity is iATPSnFR (intensity-based ATP-sensing fluorescent reporter), which allows to monitor extracellular and cytosolic ATP in HEK293 and U373 cells [170]. iATPSnFR consists in the insertion of a circularly-permutated superfolder GFP (λex/λem = 488/525 nm) between 2 α-helices of the ε subunit of the bacterial ATP synthase, as in the QUEEN biosensor. When ATP binds to the biosensor, a rapid increase in fluorescence occurs. However, iATPSnFR shows a modest pH sensitivity

which can be potentially problematic for mitochondria or other subcellular compartments that undergo significant pH variations.

Third, the intensiometric MaLion family of biosensors (Monitoring aTP Level intensiometric turn-on indicator) was used to follow cytosolic, mitochondrial and nuclear ATP levels in HeLa cells, in primary adipocytes and in *Caenorhabditis elegans* [171]. The MaLion family of biosensors consists of MaLionR, MaLionG and MaLionB, three constructs based on the fusion of the ε subunit of the bacterial ATP synthase with Red (λex/λem = 565/585 nm), Green (λex/λem = 505/522 nm) and Blue (λex/λem = 373/446 nm) fluorophores, respectively. These probes present several advantages: as for iATPSnFR, MaLionB and MaLionG were fused at their N-terminal with nuclear and mitochondrial targeting sequences for organelle-specific ATP estimations. In addition, the higher the concentration of ATP, the greater the fluorescence emission is. Last, all the probes of the family show a very low pH sensitivity.

Last, the Perceval biosensor family are ratiometric biosensors based on the estimation of the ADP/ATP ratio with live cell imaging. They are composed of a bacterial regulatory protein, GlnK1, linked to circularly permuted Venus (λex/λem = 405-490/530 nm). Similarly to the ε subunit of the bacterial ATP synthase, GlnK1 undergoes a conformational change when binding ATP. This change induces a change of the 490/405 nm ratio of cpVenus, which is proportional to ATP concentration levels. Conversely, no conformational change is observed upon ADP binding. This biosensor was validated in live mammalian cells and in yeast, and demonstrated its usefulness to determine the energy status and metabolic profiles of cells [172–175].

Overall, there is therefore a multitude of tools in the field of quantitative microscopy to measure ATP levels with high selectivity both in cells and *in vivo*. Depending on the desired detection method, but also on the model available (i.e. live cells, cell extracts, animal models etc.), it is now possible to find the most suitable sensor for any desired application (Table 1). On the other hand, rounds of optimization remain to be done in order to extend the use of these tools for diagnostic purposes.

Thanks to the thorough characterization of the probes presented in this section, it is increasingly clear that genetically-encoded biosensors present several advantages. First, they allow to work on living cells and at the single-cell level with an exquisite spatiotemporal resolution. While canonical fluorescence has a resolution limit of approximately 250 nm, FRET and BRET phenomena occur only when fluorophores are less than 10 nm apart [143,159,176]. Furthermore, the use of circularly-permutated fluorophores for ratiometric and intensiometric sensors allows to detect subtle changes in ATP production, thanks to the particular position of their chromophores within the sensors. In addition, their analysis can be performed on standard microscope setups [143].

Although genetically-encoded biosensors provide an excellent spatiotemporal resolution, they also present significant drawbacks. Among them, it is worth mentioning their non-linearity [138] and their saturation at physiological ATP levels [175]. It should also be noticed that biosensors can act as metabolite buffers, if a sensor with a low *Kd* is expressed at a high level to detect a substrate that is present at low concentrations [144,177,178]. In addition, the great majority of the fluorophores used to build biosensors are influenced by pH changes. This is why new pH-resistant fluorophores are under development, aiming to combine the benefits of standard excitation and emission wavelengths, sufficient brightness, optimal quantum yield, and a rapid maturation time together with the capacity of resisting to low pH. Last, it should be kept in mind that autofluorescence artifacts and phototoxicity in long-term experiments could potentially affect results obtained with all fluorescent-based probes, including FRET-, intensiometric, and ratiometric-based biosensors [149].

4. Conclusions and perspectives

As presented here, there is a wide range of tools available to detect and quantify ATP levels (Table 2). Historically, the first techniques implemented were biophysical approaches, such as NMR, HPLC and LC-MS/MS. These techniques have a very precise readout and allow the detection of ATP levels in denatured samples that require high quantities of starting material. However, these analyses can hardly be carried out in conventional diagnostic and/or research laboratories, mainly due to the high cost of the equipment needed to perform them. There are also biochemical techniques such as respirometry, which can indirectly measure the amount of ATP produced within mitochondria by linking ATP production to oxygen consumption in live intact cells or mitochondrial isolates. Although the possibility of using live cells is a great advance to study the concentration of ATP in its physiological environment, respirometry does not provide insights on its spatiotemporal variations.

In this light, the arrival of luminescent-based sensors (electrochemiluminescence, chemoluminescence, bioluminescence, fluorescence) has revolutionized research on ATP. The biggest benefit of these tools is that the spatiotemporal resolution of ATP levels at the single-cell scale can finally be achieved. Since ATP is largely synthesized within mitochondria, the use of an ATP synthase subunit as a mean of sensing ATP is particularly convenient.

FRET-based biosensors appear to be the most promising class of probes, as they possess a superior spatiotemporal resolution thanks to the FRET phenomenon and provide reliable quantitative information on subcellular ATP levels. However, they need to be stably or transiently integrated in the genome of the targeted cell. Chemosensors and electrochemosensors do not require an integration, but they show low specificity since the sole parameter of mitochondrial membrane potential turned out to be insufficient for their mitochondrial targeting. Single wavelength-bases biosensors are biosensors with on/off readouts, but they were shown to present a fluorescent background which makes it non-trivial to determine the off state. However, they are suitable to detect large variations in ATP production. Finally, BRET-based biosensors have a spatiotemporal resolution similar to FRET

probes, and do not require an external light source (i.e., a laser) to trigger the luciferin-luciferase reaction. In contrast to the large body of literature demonstrating the phototoxic effects of laser excitations and wavelengths on cell viability and the response of organelles to irradiations, there are very few studies exploring the effects of luciferin on cell physiology. Unless the toxic effects of luciferin are formally ruled out in future studies, FRET-based probes currently represent the best and most extensively characterized sets of probes to monitor ATP in living cells and with spatiotemporal resolution.

Defects in ATP levels and / or in ATP processing are commonly found in a variety of pathologies such as mitochondrial pathologies [179–185], chronic glaucoma [186–189], irritant dermatitis [190–192], HIV-Associated Neurocognitive Disorders (HAND) [193,194], vascular pathologies [195–201], neurodegeneratives pathologies [202–206], and cancer [207–211] . Beyond the interest of ATP as a biomarker in disease paradigms, monitoring its levels is also a valuable tool to determine the degree of contamination of surfaces in healthcare-related environments [212–216]. Overall, the need for innovative and sensitive techniques to monitor ATP levels is a major challenge for therapeutic purposes. To develop new treatments, or to improve the existing ones by limiting their side-effects [217], a deeper understanding of how metabolic homeostasis is altered in pathological conditions is mandatory. Given that cell metabolism is dynamic and highly compartimentalized, approaches that allow to simultaneously visualize different subcellular pools of ATP will certainly be of extreme interest in the near future. This will not only be important to unravel new metabolic regulations within the cell, but also to visualize the consequences of metabolic dysfunctions in patient-derived samples. In this light, robust fluorescence-based approaches combine an exquisite spatiotemporal resolution, a quantitative readout, and a high sensitivity requiring relatively low amounts of biological material. All these features are a driving force for the implementation of drug screening strategies, with the final goal of gaining a system-level understanding of metabolic alterations and therapeutic solutions for personalized medicine.

Author Contributions : S.L.N participated in the conceptualization of this review and wrote the original draft; G.B. co-conceptualized the manuscript, supervised, reviewed and finalized the manuscript.

Acknowledgments : We thank Elif Begüm Gökerküçük for helpful discussions and support. This work was supported by the *Centre National de la Recherche Scientifique* (CNRS). S.L.N. was supported by a PhD fellowship from the *Association Nationale Recherche Technologie* (ANRT) and LVMH RESEARCH. Funders have no role in manuscript preparation or revision.

References

1 Lipmann F (1975) The roots of bioenergetics. *Ciba Found Symp*, 3–22.

2 Dunn J & Grider MH (2020) Physiology, Adenosine Triphosphate. In *StatPearls* StatPearls Publishing, Treasure Island (FL).

3 Chance B, Lees H & Postgate JR (1972) The Meaning of "Reversed Electron Flow" and "High Energy Electron" in Biochemistry. *Nature* **238**, 330–331.

4 Wangler A, Schmidt C, Sadowski G & Held C (2018) Standard Gibbs Energy of Metabolic Reactions: III The 3-Phosphoglycerate Kinase Reaction. *ACS Omega* **3**, 1783–1790.

5 Pivovarov AS, Calahorro F & Walker RJ (2018) Na+/K+-pump and neurotransmitter membrane receptors. *Invert Neurosci* **19**, 1.

6 Klenchin VA & Martin TF (2000) Priming in exocytosis: attaining fusion-competence after vesicle docking. *Biochimie* **82**, 399–407.

7 Pathak D, Shields LY, Mendelsohn BA, Haddad D, Lin W, Gerencser AA, Kim H, Brand MD, Edwards RH & Nakamura K (2015) The Role of Mitochondrially Derived ATP in Synaptic Vesicle Recycling♦. *J Biol Chem* **290**, 22325–22336.

8 Sugi H (1993) Molecular Mechanism of ATP-Dependent Actin-Myosin Interaction in Muscle Contraction. *Jpn J Physiol* **43**, 435–454.

9 Bonora M, Patergnani S, Rimessi A, De Marchi E, Suski JM, Bononi A, Giorgi C, Marchi S, Missiroli S, Poletti F, Wieckowski MR & Pinton P (2012) ATP synthesis and storage. *Purinergic Signal* **8**, 343–357.

10 Schwiebert EM & Zsembery A (2003) Extracellular ATP as a signaling molecule for epithelial cells. *Biochim Biophys Acta* **1615**, 7–32.

11 Idzko M, Ferrari D & Eltzschig HK (2014) Nucleotide signalling during inflammation. *Nature* **509**, 310–317.

12 Akter S, Sharma RK, Sharma S, Rastogi S, Fiebich BL & Akundi RS Exogenous ATP modulates PGE2 release in macrophages through sustained phosphorylation of CDK9 and p38 MAPK. *J Leukoc Biol* **n/a**.

13 Novak I (2003) ATP as a signaling molecule: the exocrine focus. *News Physiol Sci Int J Physiol Prod Jointly Int Union Physiol Sci Am Physiol Soc* **18**, 12–17.

14 Burnstock G (2009) Purinergic signalling: past, present and future. *Braz J Med Biol Res* **42**, 3–8.

15 Faas MM, Sáez T & de Vos P (2017) Extracellular ATP and adenosine: The Yin and Yang in immune responses? *Mol Aspects Med* **55**, 9–19.

16 Gout E, Rébeillé F, Douce R & Bligny R (2014) Interplay of Mg2+, ADP, and ATP in the cytosol and mitochondria: Unravelling the role of Mg2+ in cell respiration. *Proc Natl Acad Sci* **111**, E4560–E4567.

17 Azarashvili TS, Odinokova IV, Krestinina OV, Baburina YL, Grachev DE, Teplova VV & Holmuhamedov EL (2011) Role of phosphorylation of porin (VDAC) in regulation of mitochondrial outer membrane under normal conditions and alcohol intoxication. *Biochem Mosc Suppl Ser Membr Cell Biol* **5**, 11–20.

18 Abeijon C, Mandon EC & Hirschberg CB (1997) Transporters of nucleotide sugars, nucleotide sulfate and ATP in the Golgi apparatus. *Trends Biochem Sci* **22**, 203–207.

19 Mayinger P, Bankaitis VA & Meyer DI (1995) Sac1p mediates the adenosine triphosphate transport into yeast endoplasmic reticulum that is required for protein translocation. *J Cell Biol* **131**, 1377–1386.

20 Haferkamp I, Fernie AR & Neuhaus HE (2011) Adenine nucleotide transport in plants: much more than a mitochondrial issue. *Trends Plant Sci* **16**, 507–515.

21 Klein M-C, Zimmermann K, Schorr S, Landini M, Klemens PAW, Altensell J, Jung M, Krause E, Nguyen D,

Helms V, Rettig J, Fecher-Trost C, Cavalié A, Hoth M, Bogeski I, Neuhaus HE, Zimmermann R, Lang S & Haferkamp I (2018) AXER is an ATP/ADP exchanger in the membrane of the endoplasmic reticulum. *Nat Commun* **9**, 3489.

22 Moriyama Y, Hiasa M, Sakamoto S, Omote H & Nomura M (2017) Vesicular nucleotide transporter (VNUT): appearance of an actress on the stage of purinergic signaling. *Purinergic Signal* **13**, 387–404.

23 Klingenberg CP (2008) Morphological Integration and Developmental Modularity. *Annu Rev Ecol Evol Syst* **39**, 115–132.

24 Nury H, Dahout-Gonzalez C, Trézéguet V, Lauquin GJM, Brandolin G & Pebay-Peyroula E (2006) Relations Between Structure and Function of the Mitochondrial ADP/ATP Carrier. *Annu Rev Biochem* **75**, 713–741.

25 Kunji ERS, Aleksandrova A, King MS, Majd H, Ashton VL, Cerson E, Springett R, Kibalchenko M, Tavoulari S, Crichton PG & Ruprecht JJ (2016) The transport mechanism of the mitochondrial ADP/ATP carrier. *Biochim Biophys Acta BBA - Mol Cell Res* **1863**, 2379–2393.

26 Kunji ERS & Ruprecht JJ (2020) The mitochondrial ADP/ATP carrier exists and functions as a monomer. *Biochem Soc Trans* **48**, 1419–1432.

27 Traba J, Satrústegui J & del Arco A (2009) Transport of adenine nucleotides in the mitochondria of Saccharomyces cerevisiae: Interactions between the ADP/ATP carriers and the ATP-Mg/Pi carrier. *Mitochondrion* **9**, 79–85.

28 Aprille JR (1993) Mechanism and regulation of the mitochondrial ATP-Mg/Pi carrier. *J Bioenerg Biomembr* **25**, 473–481.

29 Palmieri L, Santoro A, Carrari F, Blanco E, Nunes-Nesi A, Arrigoni R, Genchi F, Fernie AR & Palmieri F (2008) Identification and Characterization of ADNT1, a Novel Mitochondrial Adenine Nucleotide Transporter from Arabidopsis. *Plant Physiol* **148**, 1797–1808.

30 Zorova LD, Popkov VA, Plotnikov EY, Silachev DN, Pevzner IB, Jankauskas SS, Babenko VA, Zorov SD, Balakireva AV, Juhaszova M, Sollott SJ & Zorov DB (2018) Mitochondrial membrane potential. *Anal Biochem* **552**, 50–59.

31 Suzuki R, Hotta K & Oka K (2018) Transitional correlation between inner-membrane potential and ATP levels of neuronal mitochondria. *Sci Rep* **8**, 2993.

32 du Plessis SS, Agarwal A, Mohanty G & van der Linde M (2015) Oxidative phosphorylation versus glycolysis: what fuel do spermatozoa use? *Asian J Androl* **17**, 230–235.

33 Signes A & Fernandez-Vizarra E (2018) Assembly of mammalian oxidative phosphorylation complexes I–V and supercomplexes. *Essays Biochem* **62**, 255–270.

34 Carroll J, Fearnley IM, Skehel JM, Shannon RJ, Hirst J & Walker JE (2006) Bovine complex I is a complex of 45 different subunits. *J Biol Chem* **281**, 32724–32727.

35 Whitehouse DG Respiratory Chain and ATP Synthase. , 6.

36 Crane FL (2001) Biochemical Functions of Coenzyme Q10. *J Am Coll Nutr* **20**, 591–598.

37 Scott Mathews F (1985) The structure, function and evolution of cytochromes. *Prog Biophys Mol Biol* **45**, 1–56.

38 Wu M, Gu J, Zong S, Guo R, Liu T & Yang M (2020) Research journey of respirasome. *Protein Cell* **11**, 318–338.

39 Guo R, Gu J, Wu M & Yang M (2016) Amazing structure of respirasome: unveiling the secrets of cell respiration. *Protein Cell* **7**, 854–865.

40 Letts JA, Fiedorczuk K, Degliesposti G, Skehel M & Sazanov LA (2019) Structures of Respiratory Supercomplex I+III2 Reveal Functional and Conformational Crosstalk. *Mol Cell* **75**, 1131-1146.e6.

41 Enriquez JA & Lenaz G (2014) Coenzyme q and the respiratory chain: coenzyme q pool and mitochondrial supercomplexes. *Mol Syndromol* **5**, 119–140.
42 Woods DC (2017) Mitochondrial Heterogeneity: Evaluating Mitochondrial Subpopulation Dynamics in Stem Cells. *Stem Cells Int* **2017**, 7068567.
43 Benard G, Bellance N, James D, Parrone P, Fernandez H, Letellier T & Rossignol R (2007) Mitochondrial bioenergetics and structural network organization. *J Cell Sci* **120**, 838–848.
44 Dencher NA, Frenzel M, Reifschneider NH, Sugawa M & Krause F (2007) Proteome alterations in rat mitochondria caused by aging. *Ann N Y Acad Sci* **1100**, 291–298.
45 Helbig AO, de Groot MJL, van Gestel RA, Mohammed S, de Hulster EAF, Luttik MAH, Daran-Lapujade P, Pronk JT, Heck AJR & Slijper M (2009) A three-way proteomics strategy allows differential analysis of yeast mitochondrial membrane protein complexes under anaerobic and aerobic conditions. *Proteomics* **9**, 4787–4798.
46 Ramírez-Aguilar SJ, Keuthe M, Rocha M, Fedyaev VV, Kramp K, Gupta KJ, Rasmusson AG, Schulze WX & van Dongen JT (2011) The Composition of Plant Mitochondrial Supercomplexes Changes with Oxygen Availability. *J Biol Chem* **286**, 43045–43053.
47 Cogliati S, Frezza C, Soriano ME, Varanita T, Quintana-Cabrera R, Corrado M, Cipolat S, Costa V, Casarin A, Gomes LC, Perales-Clemente E, Salviati L, Fernandez-Silva P, Enriquez JA & Scorrano L (2013) Mitochondrial Cristae Shape Determines Respiratory Chain Supercomplexes Assembly and Respiratory Efficiency. *Cell* **155**, 160–171.
48 Greggio C, Jha P, Kulkarni SS, Lagarrigue S, Broskey NT, Boutant M, Wang X, Conde Alonso S, Ofori E, Auwerx J, Cantó C & Amati F (2017) Enhanced Respiratory Chain Supercomplex Formation in Response to Exercise in Human Skeletal Muscle. *Cell Metab* **25**, 301–311.
49 Jang S, Lewis TS, Powers C, Khuchua Z, Baines CP, Wipf P & Javadov S (2017) Elucidating Mitochondrial Electron Transport Chain Supercomplexes in the Heart During Ischemia–Reperfusion. *Antioxid Redox Signal* **27**, 57–69.
50 Rosca MG, Vazquez EJ, Kerner J, Parland W, Chandler MP, Stanley W, Sabbah HN & Hoppel CL (2008) Cardiac mitochondria in heart failure: decrease in respirasomes and oxidative phosphorylation. *Cardiovasc Res* **80**, 30–39.
51 Sousa JS, Mills DJ, Vonck J & Kühlbrandt W (2016) Functional asymmetry and electron flow in the bovine respirasome. *eLife* **5**, e21290.
52 Hirst J (2018) Open questions: respiratory chain supercomplexes—why are they there and what do they do? *BMC Biol* **16**, 111.
53 Habersetzer J, Ziani W, Larrieu I, Stines-Chaumeil C, Giraud M-F, Brèthes D, Dautant A & Paumard P (2013) ATP synthase oligomerization: from the enzyme models to the mitochondrial morphology. *Int J Biochem Cell Biol* **45**, 99–105.
54 Wittig I, Meyer B, Heide H, Steger M, Bleier L, Wumaier Z, Karas M & Schägger H (2010) Assembly and oligomerization of human ATP synthase lacking mitochondrial subunits a and A6L. *Biochim Biophys Acta* **1797**, 1004–1011.
55 Martijn J, Vosseberg J, Guy L, Offre P & Ettema TJG (2018) Deep mitochondrial origin outside the sampled alphaproteobacteria. *Nature* **557**, 101–105.
56 Gabaldón T (2018) Relative timing of mitochondrial endosymbiosis and the "pre-mitochondrial symbioses" hypothesis. *IUBMB Life* **70**, 1188–1196.
57 Gray MW (2017) Lynn Margulis and the endosymbiont hypothesis: 50 years later. *Mol Biol Cell* **28**, 1285–1287.

58 Roger AJ, Muñoz-Gómez SA & Kamikawa R (2017) The Origin and Diversification of Mitochondria. *Curr Biol CB* **27**, R1177–R1192.
59 Pavlov E, Aschar-Sobbi R, Campanella M, Turner RJ, Gómez-García MR & Abramov AY (2010) Inorganic Polyphosphate and Energy Metabolism in Mammalian Cells. *J Biol Chem* **285**, 9420–9428.
60 Achbergerová L & Nahálka J (2011) Polyphosphate - an ancient energy source and active metabolic regulator. *Microb Cell Factories* **10**, 63.
61 Kornberg A (1999) Inorganic Polyphosphate: A Molecule of Many Functions. In *Inorganic Polyphosphates* (Schröder HC & Müller WEG, eds), pp. 1–18. Springer Berlin Heidelberg, Berlin, Heidelberg.
62 Seidlmayer LK, Gomez-Garcia MR, Shiba T, Porter GA, Pavlov EV, Bers DM & Dedkova EN (2019) Dual role of inorganic polyphosphate in cardiac myocytes: The importance of polyP chain length for energy metabolism and mPTP activation. *Arch Biochem Biophys* **662**, 177–189.
63 Dedkova EN & Blatter LA (2014) Role of β-hydroxybutyrate, its polymer poly-β-hydroxybutyrate and inorganic polyphosphate in mammalian health and disease. *Front Physiol* **0**.
64 Gray MW (2012) Mitochondrial Evolution. *Cold Spring Harb Perspect Biol* **4**.
65 Gray MW (2014) The pre-endosymbiont hypothesis: a new perspective on the origin and evolution of mitochondria. *Cold Spring Harb Perspect Biol* **6**.
66 Morelli A & Rosano C (2016) A True Symbiosis for the Mitochondria Evolution. *Bioenerg Open Access* **05**.
67 Guo H, Suzuki T & Rubinstein JL (2019) Structure of a bacterial ATP synthase. *eLife* **8**.
68 Dabbeni-Sala F, Rai AK & Lippe G (2012) F0F1 ATP Synthase: A Fascinating Challenge for Proteomics. *Proteomics - Hum Dis Protein Funct*.
69 He J, Ford HC, Carroll J, Douglas C, Gonzales E, Ding S, Fearnley IM & Walker JE (2018) Assembly of the membrane domain of ATP synthase in human mitochondria. *Proc Natl Acad Sci* **115**, 2988–2993.
70 Xu T, Pagadala V & Mueller DM (2015) Understanding structure, function, and mutations in the mitochondrial ATP synthase. *Microb Cell Graz Austria* **2**, 105–125.
71 Menz RI, Walker JE & Leslie AG (2001) Structure of bovine mitochondrial F(1)-ATPase with nucleotide bound to all three catalytic sites: implications for the mechanism of rotary catalysis. *Cell* **106**, 331–341.
72 Sobti M, Ueno H, Noji H & Stewart AG (2020) The six steps of the F1-ATPase rotary catalytic cycle. *bioRxiv*, 2020.12.15.422962.
73 Giorgio V, von Stockum S, Antoniel M, Fabbro A, Fogolari F, Forte M, Glick GD, Petronilli V, Zoratti M, Szabó I, Lippe G & Bernardi P (2013) Dimers of mitochondrial ATP synthase form the permeability transition pore. *Proc Natl Acad Sci U S A* **110**, 5887–5892.
74 Carraro M, Checchetto V, Szabó I & Bernardi P (2019) F-ATP synthase and the permeability transition pore: fewer doubts, more certainties. *FEBS Lett* **593**, 1542–1553.
75 Bonora M, Bononi A, De Marchi E, Giorgi C, Lebiedzinska M, Marchi S, Patergnani S, Rimessi A, Suski JM, Wojtala A, Wieckowski MR, Kroemer G, Galluzzi L & Pinton P (2013) Role of the c subunit of the FO ATP synthase in mitochondrial permeability transition. *Cell Cycle* **12**, 674–683.
76 Alavian KN, Beutner G, Lazrove E, Sacchetti S, Park H-A, Licznerski P, Li H, Nabili P, Hockensmith K, Graham M, Porter GA & Jonas EA (2014) An uncoupling channel within the c-subunit ring of the F1FO ATP synthase is the mitochondrial permeability transition pore. *Proc Natl Acad Sci U S A* **111**, 10580–10585.
77 Bernardi P (2020) Mechanisms for Ca2+-dependent permeability transition in mitochondria. *Proc Natl Acad Sci U S A* **117**, 2743–2744.
78 Gerle C (2020) Mitochondrial F-ATP synthase as the permeability transition pore. *Pharmacol Res* **160**, 105081.
79 Bauer Tyler M. & Murphy Elizabeth (2020) Role of Mitochondrial Calcium and the Permeability Transition

Pore in Regulating Cell Death. *Circ Res* **126**, 280–293.
80 Shanmughapriya S, Rajan S, Hoffman NE, Higgins AM, Tomar D, Nemani N, Hines KJ, Smith DJ, Eguchi A, Vallem S, Shaikh F, Cheung M, Leonard NJ, Stolakis RS, Wolfers MP, Ibetti J, Chuprun JK, Jog NR, Houser SR, Koch WJ, Elrod JW & Madesh M (2015) SPG7 is an Essential and Conserved Component of the Mitochondrial Permeability Transition Pore. *Mol Cell* **60**, 47–62.
81 Rottenberg H & Hoek JB (2021) The Mitochondrial Permeability Transition: Nexus of Aging, Disease and Longevity. *Cells* **10**, 79.
82 Winquist RJ & Gribkoff VK (2020) Targeting putative components of the mitochondrial permeability transition pore for novel therapeutics. *Biochem Pharmacol* **177**, 113995.
83 Ko YH, Delannoy M, Hullihen J, Chiu W & Pedersen PL (2003) Mitochondrial ATP synthasome. Cristae-enriched membranes and a multiwell detergent screening assay yield dispersed single complexes containing the ATP synthase and carriers for Pi and ADP/ATP. *J Biol Chem* **278**, 12305–12309.
84 Chen C, Ko Y, Delannoy M, Ludtke SJ, Chiu W & Pedersen PL (2004) Mitochondrial ATP synthasome: three-dimensional structure by electron microscopy of the ATP synthase in complex formation with carriers for Pi and ADP/ATP. *J Biol Chem* **279**, 31761–31768.
85 Nůsková H, Mráček T, Mikulová T, Vrbacký M, Kovářová N, Kovalčíková J, Pecina P & Houštěk J (2015) Mitochondrial ATP synthasome: Expression and structural interaction of its components. *Biochem Biophys Res Commun* **464**, 787–793.
86 Belosludtsev KN, Dubinin MV, Belosludtseva NV & Mironova GD (2019) Mitochondrial Ca2+ Transport: Mechanisms, Molecular Structures, and Role in Cells. *Biochem Biokhimiia* **84**, 593–607.
87 Belosludtsev KN, Dubinin MV, Talanov EY, Starinets VS, Tenkov KS, Zakharova NM & Belosludtseva NV (2020) Transport of Ca2+ and Ca2+-Dependent Permeability Transition in the Liver and Heart Mitochondria of Rats with Different Tolerance to Acute Hypoxia. *Biomolecules* **10**.
88 Belosludtsev KN, Talanov EY, Starinets VS, Agafonov AV, Dubinin MV & Belosludtseva NV (2019) Transport of Ca2+ and Ca2+-Dependent Permeability Transition in Rat Liver Mitochondria under the Streptozotocin-Induced Type I Diabetes. *Cells* **8**.
89 Bernardi P, Rasola A, Forte M & Lippe G (2015) The Mitochondrial Permeability Transition Pore: Channel Formation by F-ATP Synthase, Integration in Signal Transduction, and Role in Pathophysiology. *Physiol Rev* **95**, 1111–1155.
90 Turunen M, Olsson J & Dallner G (2004) Metabolism and function of coenzyme Q. *Biochim Biophys Acta BBA - Biomembr* **1660**, 171–199.
91 Javadov S, Jang S, Parodi-Rullan R, Khuchua Z & Kuznetsov AV (2017) Mitochondrial permeability transition in cardiac ischemia–reperfusion: whether cyclophilin D is a viable target for cardioprotection? *Cell Mol Life Sci CMLS* **74**, 2795–2813.
92 Rasola A & Bernardi P (2014) The mitochondrial permeability transition pore and its adaptive responses in tumor cells. *Cell Calcium* **56**, 437–445.
93 Mlynárik V (2017) Introduction to nuclear magnetic resonance. *Anal Biochem* **529**, 4–9.
94 Sersa I, Kranjc S, Sersa G, Nemec-Svete A, Lozar B, Sepe A, Vidmar J & Sentjurc M (2010) Study of radiation induced changes of phosphorus metabolism in mice by (31)P NMR spectroscopy. *Radiol Oncol* **44**, 174–179.
95 Guo B, Gurel PS, Shu R, Higgs HN, Pellegrini M & Mierke DF (2014) Monitoring ATP hydrolysis and ATPase inhibitor screening using 1H NMR. *Chem Commun Camb Engl* **50**, 12037–12039.
96 Lian Y, Jiang H, Feng J, Wang X, Hou X & Deng P (2016) Direct and simultaneous quantification of ATP, ADP and AMP by (1)H and (31)P Nuclear Magnetic Resonance spectroscopy. *Talanta* **150**, 485–492.

97 Holzgrabe U, Deubner R, Schollmayer C & Waibel B (2005) Quantitative NMR spectroscopy—Applications in drug analysis. *J Pharm Biomed Anal* **38**, 806–812.
98 Trams EG, Kaufmann H & Burnstock G (1980) A proposal for the role of ecto-enzymes and adenylates in traumatic shock. *J Theor Biol* **87**, 609–621.
99 Kudisch B, Maiuri M, Moretti L, Oviedo MB, Wang L, Oblinsky DG, Prud'homme RK, Wong BM, McGill SA & Scholes GD (2020) Ring currents modulate optoelectronic properties of aromatic chromophores at 25 T. *Proc Natl Acad Sci* **117**, 11289–11298.
100 Parker T, Limer E, Watson AD, Defernez M, Williamson D & Kemsley EK (2014) 60 MHz 1H NMR spectroscopy for the analysis of edible oils. *Trends Anal Chem* **57**, 147–158.
101 Quine RW, Rinard GA, Shi Y, Buchanan L, Biller JR, Eaton SS & Eaton GR (2016) UHF EPR spectrometer operating at frequencies between 400 MHz and 1 GHz. *Concepts Magn Reson Part B Magn Reson Eng* **46B**, 123–133.
102 Blum F (2014) High performance liquid chromatography. *Br J Hosp Med Lond Engl 2005* **75**, C18-21.
103 Liu H, Jiang Y, Luo Y & Jiang W (2006) A Simple and Rapid Determination of ATP, ADP and AMP Concentrations in Pericarp Tissue of Litchi Fruit by High Performance Liquid Chromatography. , 4.
104 Menegollo M, Tessari I, Bubacco L & Szabadkai G (2019) Determination of ATP, ADP, and AMP Levels by Reversed-Phase High-Performance Liquid Chromatography in Cultured Cells. *Methods Mol Biol Clifton NJ* **1925**, 223–232.
105 von Papen M, Gambaryan S, Schütz C & Geiger J (2013) Determination of ATP and ADP Secretion from Human and Mouse Platelets by an HPLC Assay. *Transfus Med Hemotherapy Off Organ Dtsch Ges Transfusionsmedizin Immunhamatologie* **40**, 109–116.
106 Bhatt DP, Chen X, Geiger JD & Rosenberger TA (2012) A sensitive HPLC-based method to quantify adenine nucleotides in primary astrocyte cell cultures. *J Chromatogr B Analyt Technol Biomed Life Sci* **889–890**, 110–115.
107 Pitt JJ (2009) Principles and Applications of Liquid Chromatography-Mass Spectrometry in Clinical Biochemistry. *Clin Biochem Rev* **30**, 19–34.
108 Fu X, Deja S, Kucejova B, Duarte JAG, McDonald JG & Burgess SC (2019) Targeted Determination of Tissue Energy Status by LC-MS/MS. *Anal Chem* **91**, 5881–5887.
109 Kim H, Kosinski P, Kung C, Dang L, Chen Y, Yang H, Chen Y-S, Kramer J & Liu G (2017) A fit-for-purpose LC-MS/MS method for the simultaneous quantitation of ATP and 2,3-DPG in human K2EDTA whole blood. *J Chromatogr B Analyt Technol Biomed Life Sci* **1061–1062**, 89–96.
110 Djafarzadeh S & Jakob SM (2017) High-resolution Respirometry to Assess Mitochondrial Function in Permeabilized and Intact Cells. *J Vis Exp JoVE*.
111 Horan MP, Pichaud N & Ballard JWO (2012) Review: Quantifying Mitochondrial Dysfunction in Complex Diseases of Aging. *J Gerontol Ser A* **67**, 1022–1035.
112 Rose S, Carvalho E, Diaz EC, Cotter M, Bennuri SC, Azhar G, Frye RE, Adams SH & Børsheim E (2019) A comparative study of mitochondrial respiration in circulating blood cells and skeletal muscle fibers in women. *Am J Physiol-Endocrinol Metab* **317**, E503–E512.
113 Rogers GW, Brand MD, Petrosyan S, Ashok D, Elorza AA, Ferrick DA & Murphy AN (2011) High throughput microplate respiratory measurements using minimal quantities of isolated mitochondria. *PloS One* **6**, e21746.
114 Devenish RJ, Prescott M, Boyle GM & Nagley P (2000) The oligomycin axis of mitochondrial ATP synthase: OSCP and the proton channel. *J Bioenerg Biomembr* **32**, 507–515.
115 Benz R & McLaughlin S (1983) The molecular mechanism of action of the proton ionophore FCCP

(carbonylcyanide p-trifluoromethoxyphenylhydrazone). *Biophys J* **41**, 381–398.
116 Ma X, Jin M, Cai Y, Xia H, Long K, Liu J, Yu Q & Yuan J (2011) Mitochondrial Electron Transport Chain Complex III Is Required for Antimycin A to Inhibit Autophagy. *Chem Biol* **18**, 1474–81.
117 Heinz S, Freyberger A, Lawrenz B, Schladt L, Schmuck G & Ellinger-Ziegelbauer H (2017) Mechanistic Investigations of the Mitochondrial Complex I Inhibitor Rotenone in the Context of Pharmacological and Safety Evaluation. *Sci Rep* **7**.
118 Liu Y, Gu Y & Yu X (2017) Assessing tissue metabolism by phosphorous-31 magnetic resonance spectroscopy and imaging: a methodology review. *Quant Imaging Med Surg* **7**, 707–726.
119 Walchhofer LM, Steiger R, Rietzler A, Kerschbaumer J, Freyschlag CF, Stockhammer G, Gizewski ER & Grams AE (2021) Phosphorous Magnetic Resonance Spectroscopy to Detect Regional Differences of Energy and Membrane Metabolism in Naïve Glioblastoma Multiforme. *Cancers* **13**, 2598.
120 Blazek M, Santisteban TS, Zengerle R & Meier M (2015) Analysis of fast protein phosphorylation kinetics in single cells on a microfluidic chip. *Lab Chip* **15**, 726–734.
121 Kobayashi H, Ogawa M, Alford R, Choyke PL & Urano Y (2010) New strategies for fluorescent probe design in medical diagnostic imaging. *Chem Rev* **110**, 2620–2640.
122 Wu Y, Wen J, Li H, Sun S & Xu Y (2017) Fluorescent probes for recognition of ATP. *Chin Chem Lett* **28**, 1916–1924.
123 Liu Y, Lei J, Huang Y & Ju H (2014) "Off-on" electrochemiluminescence system for sensitive detection of ATP via target-induced structure switching. *Anal Chem* **86**, 8735–8741.
124 Liu B, Cui Y, Tang D, Yang H & Chen G (2012) Au(III)-assisted core–shell iron oxide@poly(o-phenylenediamine) nanostructures for ultrasensitive electrochemical aptasensors based on DNase I-catalyzed target recycling. *Chem Commun* **48**, 2624–2626.
125 Yin B-C, Guan Y-M & Ye B-C (2012) An ultrasensitive electrochemical DNA sensor based on the ssDNA-assisted cascade of hybridization reaction. *Chem Commun* **48**, 4208–4210.
126 Ho Y-P & Leong KW (2010) Quantum dot-based theranostics. *Nanoscale* **2**, 60–68.
127 Pleskova S, Mikheeva E & Gornostaeva E (2018) Using of Quantum Dots in Biology and Medicine. *Adv Exp Med Biol* **1048**, 323–334.
128 Jaiswal JK, Goldman ER, Mattoussi H & Simon SM (2004) Use of quantum dots for live cell imaging. *Nat Methods* **1**, 73–78.
129 Xu Z, Zeng G, Liu Y, Zhang X, Cheng J, Zhang J, Ma Z, Miao M, Zhang D & Wei Y (2019) Monitoring mitochondrial ATP in live cells: An ATP multisite-binding fluorescence turn-on probe. *Dyes Pigments* **163**, 559–563.
130 Reungpatthanaphong P, Dechsupa S, Meesungnoen J, Loetchutinat C & Mankhetkorn S (2003) Rhodamine B as a mitochondrial probe for measurement and monitoring of mitochondrial membrane potential in drug-sensitive and -resistant cells. *J Biochem Biophys Methods* **57**, 1–16.
131 Wang L, Yuan L, Zeng X, Peng J, Ni Y, Er JC, Xu W, Agrawalla BK, Su D, Kim B & Chang Y-T (2016) A Multisite-Binding Switchable Fluorescent Probe for Monitoring Mitochondrial ATP Level Fluctuation in Live Cells. *Angew Chem Int Ed Engl* **55**, 1773–1776.
132 Tan K-Y, Li C-Y, Li Y-F, Fei J, Yang B, Fu Y-J & Li F (2017) Real-Time Monitoring ATP in Mitochondrion of Living Cells: A Specific Fluorescent Probe for ATP by Dual Recognition Sites. *Anal Chem* **89**, 1749–1756.
133 Liu Y, Lee D, Wu D, Swamy KMK & Yoon J (2018) A new kind of rhodamine-based fluorescence turn-on probe for monitoring ATP in mitochondria. *Sens Actuators B Chem* **265**, 429–434.
134 Gao J-Y, Huang W-C, Huang P-Y, Song C-Y & Hong J-L (2017) Light-Up of Rhodamine Hydrazide to

Generate Emissive Initiator for Polymerization and to Afford Photochromic Polypeptide Metal Complex. *Polymers* **9**.

135 Dittrich M, Hayashi S & Schulten K (2003) On the Mechanism of ATP Hydrolysis in F1-ATPase. *Biophys J* **85**, 2253–2266.

136 Kato-Yamada Y & Yoshida M (2003) Isolated epsilon subunit of thermophilic F1-ATPase binds ATP. *J Biol Chem* **278**, 36013–36016.

137 Yagi H, Kajiwara N, Tanaka H, Tsukihara T, Kato-Yamada Y, Yoshida M & Akutsu H (2007) Structures of the thermophilic F1-ATPase epsilon subunit suggesting ATP-regulated arm motion of its C-terminal domain in F1. *Proc Natl Acad Sci U S A* **104**, 11233–11238.

138 Imamura H, Nhat KPH, Togawa H, Saito K, Iino R, Kato-Yamada Y, Nagai T & Noji H (2009) Visualization of ATP levels inside single living cells with fluorescence resonance energy transfer-based genetically encoded indicators. *Proc Natl Acad Sci* **106**, 15651–15656.

139 Iino R, Murakami T, Iizuka S, Kato-Yamada Y, Suzuki T & Yoshida M (2005) Real-time monitoring of conformational dynamics of the epsilon subunit in F1-ATPase. *J Biol Chem* **280**, 40130–40134.

140 Campbell RE (2009) Fluorescent-protein-based biosensors: modulation of energy transfer as a design principle. *Anal Chem* **81**, 5972–5979.

141 Tsuyama T, Kishikawa J, Han Y-W, Harada Y, Tsubouchi A, Noji H, Kakizuka A, Yokoyama K, Uemura T & Imamura H (2013) In vivo fluorescent adenosine 5'-triphosphate (ATP) imaging of Drosophila melanogaster and Caenorhabditis elegans by using a genetically encoded fluorescent ATP biosensor optimized for low temperatures. *Anal Chem* **85**, 7889–7896.

142 Yoshida T, Alfaqaan S, Sasaoka N & Imamura H (2017) Application of FRET-Based Biosensor "ATeam" for Visualization of ATP Levels in the Mitochondrial Matrix of Living Mammalian Cells. In *Mitochondria* (Mokranjac D & Perocchi F, eds), pp. 231–243. Springer New York, New York, NY.

143 Padilla-Parra S & Tramier M (2012) FRET microscopy in the living cell: Different approaches, strengths and weaknesses. *BioEssays* **34**, 369–376.

144 Liemburg-Apers DC, Imamura H, Forkink M, Nooteboom M, Swarts HG, Brock R, Smeitink JAM, Willems PHGM & Koopman WJH (2011) Quantitative Glucose and ATP Sensing in Mammalian Cells. *Pharm Res* **28**, 2745–2757.

145 Depaoli MR, Karsten F, Madreiter-Sokolowski CT, Klec C, Gottschalk B, Bischof H, Eroglu E, Waldeck-Weiermair M, Simmen T, Graier WF & Malli R (2018) Real-Time Imaging of Mitochondrial ATP Dynamics Reveals the Metabolic Setting of Single Cells. *Cell Rep* **25**, 501-512.e3.

146 Morciano G, Sarti AC, Marchi S, Missiroli S, Falzoni S, Raffaghello L, Pistoia V, Giorgi C, Di Virgilio F & Pinton P (2017) Use of luciferase probes to measure ATP in living cells and animals. *Nat Protoc* **12**, 1542–1562.

147 Conley JM, Radhakrishnan S, Valentino SA & Tantama M (2017) Imaging extracellular ATP with a genetically-encoded, ratiometric fluorescent sensor. *PloS One* **12**, e0187481.

148 Vishnu N, Jadoon Khan M, Karsten F, Groschner LN, Waldeck-Weiermair M, Rost R, Hallström S, Imamura H, Graier WF & Malli R (2014) ATP increases within the lumen of the endoplasmic reticulum upon intracellular Ca2+ release. *Mol Biol Cell* **25**, 368–379.

149 Nakano M, Imamura H, Nagai T & Noji H (2011) Ca^{2+} regulation of mitochondrial ATP synthesis visualized at the single cell level. *ACS Chem Biol* **6**, 709–715.

150 Douthwright S & Sluder G (2017) Live Cell Imaging: Assessing the Phototoxicity of 488 and 546 nm Light and Methods to Alleviate it. *J Cell Physiol* **232**, 2461–2468.

151 Zadran S, Sanchez D, Zadran H, Amighi A, Otiniano E & Wong K (2013) Enhanced-acceptor fluorescence-

based single cell ATP biosensor monitors ATP in heterogeneous cancer populations in real time. *Biotechnol Lett* **35**, 175–180.
152 Inouye S (2010) Firefly luciferase: an adenylate-forming enzyme for multicatalytic functions. *Cell Mol Life Sci CMLS* **67**, 387–404.
153 Holmsen H, Storm E & Day HJ (1972) Determination of ATP and ADP in blood platelets: a modification of the firefly luciferase assay for plasma. *Anal Biochem* **46**, 489–501.
154 Kimmich GA, Randles J & Brand JS (1975) Assay of picomole amounts of ATP, ADP, and AMP using the luciferase enzyme system. *Anal Biochem* **69**, 187–206.
155 Rangaraju V, Calloway N & Ryan TA (2014) Activity-driven local ATP synthesis is required for synaptic function. *Cell* **156**, 825–835.
156 Min K & Steghens J (2001) ADP is produced by firefly luciferase but its synthesis is independent of the light emitting properties. *Biochimie* **83**, 523–528.
157 Lemasters JJ & Hackenbrock CR (1978) [4] Firefly luciferase assay for ATP production by mitochondria. In *Methods in Enzymology* pp. 36–50. Academic Press.
158 Brown NE, Blumer JB & Hepler JR (2015) Bioluminescence Resonance Energy Transfer to Detect Protein-Protein Interactions in Live Cells. *Methods Mol Biol Clifton NJ* **1278**, 457–465.
159 Yoshida T, Kakizuka A & Imamura H (2016) BTeam, a Novel BRET-based Biosensor for the Accurate Quantification of ATP Concentration within Living Cells. *Sci Rep* **6**, 39618.
160 Saito K, Chang Y-F, Horikawa K, Hatsugai N, Higuchi Y, Hashida M, Yoshida Y, Matsuda T, Arai Y & Nagai T (2012) Luminescent proteins for high-speed single-cell and whole-body imaging. *Nat Commun* **3**, 1262.
161 Min S-H, French AR, Trull KJ, Tat K, Varney SA & Tantama M (2019) Ratiometric BRET Measurements of ATP with a Genetically-Encoded Luminescent Sensor. *Sensors* **19**.
162 Dagogo-Jack I & Shaw AT (2018) Tumour heterogeneity and resistance to cancer therapies. *Nat Rev Clin Oncol* **15**, 81–94.
163 Arts R, Aper SJA & Merkx M (2017) Engineering BRET-Sensor Proteins. *Methods Enzymol* **589**, 87–114.
164 Ignowski JM & Schaffer DV (2004) Kinetic analysis and modeling of firefly luciferase as a quantitative reporter gene in live mammalian cells. *Biotechnol Bioeng* **86**, 827–834.
165 Kumar JS, Miller Jenkins LM, Gottesman MM & Hall MD (2016) The Drug Excipient Cyclodextrin Interacts With d-Luciferin and Interferes With Bioluminescence Imaging. *Mol Imaging* **15**.
166 Takakura H, Sasakura K, Ueno T, Urano Y, Terai T, Hanaoka K, Tsuboi T & Nagano T (2010) Development of luciferin analogues bearing an amino group and their application as BRET donors. *Chem Asian J* **5**, 2053–2061.
167 Weihs F & Dacres H (2019) Red-shifted bioluminescence Resonance Energy Transfer: Improved tools and materials for analytical in vivo approaches. *TrAC Trends Anal Chem* **116**, 61–73.
168 Kostyuk AI, Demidovich AD, Kotova DA, Belousov VV & Bilan DS (2019) Circularly Permuted Fluorescent Protein-Based Indicators: History, Principles, and Classification. *Int J Mol Sci* **20**.
169 Yaginuma H, Kawai S, Tabata KV, Tomiyama K, Kakizuka A, Komatsuzaki T, Noji H & Imamura H (2014) Diversity in ATP concentrations in a single bacterial cell population revealed by quantitative single-cell imaging. *Sci Rep* **4**, 6522.
170 Lobas MA, Tao R, Nagai J, Kronschläger MT, Borden PM, Marvin JS, Looger LL & Khakh BS (2019) A genetically encoded single-wavelength sensor for imaging cytosolic and cell surface ATP. *Nat Commun* **10**, 711.
171 Arai S, Kriszt R, Harada K, Looi L-S, Matsuda S, Wongso D, Suo S, Ishiura S, Tseng Y-H, Raghunath M, Ito T, Tsuboi T & Kitaguchi T (2018) RGB-Color Intensiometric Indicators to Visualize Spatiotemporal Dynamics of ATP in Single Cells. *Angew Chem Int Ed Engl* **57**, 10873–10878.

172 Nguyen PTM, Ishiwata-Kimata Y & Kimata Y (2019) Monitoring ADP/ATP ratio in yeast cells using the fluorescent-protein reporter PercevalHR. *Biosci Biotechnol Biochem* **83**, 824–828.
173 Tarasov AI & Rutter GA (2014) Use of genetically encoded sensors to monitor cytosolic ATP/ADP ratio in living cells. *Methods Enzymol* **542**, 289–311.
174 Tantama M, Martínez-François JR, Mongeon R & Yellen G (2013) Imaging energy status in live cells with a fluorescent biosensor of the intracellular ATP-to-ADP ratio. *Nat Commun* **4**, 2550.
175 Berg J, Hung YP & Yellen G (2009) A genetically encoded fluorescent reporter of ATP:ADP ratio. *Nat Methods* **6**, 161–166.
176 Zadran S, Standley S, Wong K, Otiniano E, Amighi A & Baudry M (2012) Fluorescence resonance energy transfer (FRET)-based biosensors: visualizing cellular dynamics and bioenergetics. *Appl Microbiol Biotechnol* **96**, 895–902.
177 De Col V, Fuchs P, Nietzel T, Elsässer M, Voon CP, Candeo A, Seeliger I, Fricker MD, Grefen C, Møller IM, Bassi A, Lim BL, Zancani M, Meyer AJ, Costa A, Wagner S & Schwarzländer M (2017) ATP sensing in living plant cells reveals tissue gradients and stress dynamics of energy physiology. *eLife* **6**, e26770.
178 McMahon SM & Jackson MB (2018) An Inconvenient Truth: Calcium Sensors Are Calcium Buffers. *Trends Neurosci* **41**, 880–884.
179 Kucharczyk R, Zick M, Bietenhader M, Rak M, Couplan E, Blondel M, Caubet S-D & di Rago J-P (2009) Mitochondrial ATP synthase disorders: molecular mechanisms and the quest for curative therapeutic approaches. *Biochim Biophys Acta* **1793**, 186–199.
180 DiMauro S & Mancuso M (2007) Mitochondrial diseases: therapeutic approaches. *Biosci Rep* **27**, 125–137.
181 Mikol J & Polivka M (2005) [Mitochondrial encephalomyopathies]. *Ann Pathol* **25**, 282–291.
182 Janssen RJRJ, van den Heuvel LP & Smeitink JAM (2004) Genetic defects in the oxidative phosphorylation (OXPHOS) system. *Expert Rev Mol Diagn* **4**, 143–156.
183 Smeitink J, van den Heuvel L & DiMauro S (2001) The genetics and pathology of oxidative phosphorylation. *Nat Rev Genet* **2**, 342–352.
184 Rizza T, Vazquez-Memije ME, Meschini MC, Bianchi M, Tozzi G, Nesti C, Piemonte F, Bertini E, Santorelli FM & Carrozzo R (2009) Assaying ATP synthesis in cultured cells: a valuable tool for the diagnosis of patients with mitochondrial disorders. *Biochem Biophys Res Commun* **383**, 58–62.
185 Dubinin MV, Talanov EY, Tenkov KS, Starinets VS, Belosludtseva NV & Belosludtsev KN (2020) The Effect of Deflazacort Treatment on the Functioning of Skeletal Muscle Mitochondria in Duchenne Muscular Dystrophy. *Int J Mol Sci* **21**.
186 Weinreb RN, Aung T & Medeiros FA (2014) The pathophysiology and treatment of glaucoma: a review. *JAMA* **311**, 1901–1911.
187 Lu W, Hu H, Sévigny J, Gabelt BT, Kaufman PL, Johnson EC, Morrison JC, Zode GS, Sheffield VC, Zhang X, Laties AM & Mitchell CH (2015) Rat, mouse, and primate models of chronic glaucoma show sustained elevation of extracellular ATP and altered purinergic signaling in the posterior eye. *Invest Ophthalmol Vis Sci* **56**, 3075–3083.
188 Stamer WD (2015) Implications of sustained elevation in extracellular ATP in retina following chronic ocular hypertension. *Invest Ophthalmol Vis Sci* **56**, 3084.
189 Ju W-K, Kim K-Y, Lindsey JD, Angert M, Duong-Polk KX, Scott RT, Kim JJ, Kukhmazov I, Ellisman MH, Perkins GA & Weinreb RN (2008) Intraocular pressure elevation induces mitochondrial fission and triggers OPA1 release in glaucomatous optic nerve. *Invest Ophthalmol Vis Sci* **49**, 4903–4911.
190 Zanin RF, da Silva GL, Erig T, Sperotto NDM, Leite CE, Coutinho-Silva R, Batastini AMO & Morrone FB

(2015) Decrease of serum adenine nucleotide hydrolysis in an irritant contact dermatitis mice model: potential P2X7R involvement. *Mol Cell Biochem* **404**, 221–228.
191 Lee HY, Stieger M, Yawalkar N & Kakeda M (2013) Cytokines and chemokines in irritant contact dermatitis. *Mediators Inflamm* **2013**, 916497.
192 Mizumoto N, Mummert ME, Shalhevet D & Takashima A (2003) Keratinocyte ATP Release Assay for Testing Skin-Irritating Potentials of Structurally Diverse Chemicals. *J Invest Dermatol* **121**, 1066–1072.
193 Velasquez S, Prevedel L, Valdebenito S, Gorska AM, Golovko M, Khan N, Geiger J & Eugenin EA (2020) Circulating levels of ATP is a biomarker of HIV cognitive impairment. *EBioMedicine* **51**, 102503.
194 Gendelman HE (2020) Predictive biomarkers for cognitive decline during progressive HIV infection. *EBioMedicine* **51**, 102538.
195 Guth CM, Luo W, Jolayemi O, Chadalavada KS, Komalavilas P, Cheung-Flynn J & Brophy CM (2017) Adenosine triphosphate as a molecular mediator of the vascular response to injury. *J Surg Res* **216**, 80–86.
196 Zhang H, Shen Z, Hogan B, Barakat AI & Misbah C (2018) ATP Release by Red Blood Cells under Flow: Model and Simulations. *Biophys J* **115**, 2218–2229.
197 Yeung PK, Kolathuru SS, Mohammadizadeh S, Akhoundi F & Linderfield B (2018) Adenosine 5'-Triphosphate Metabolism in Red Blood Cells as a Potential Biomarker for Post-Exercise Hypotension and a Drug Target for Cardiovascular Protection. *Metabolites* **8**.
198 Li Y, Zhou J, Burkovskiy I, Yeung P & Lehmann C (2019) ATP in red blood cells as biomarker for sepsis in humans. *Med Hypotheses* **124**, 84–86.
199 Farthing DE, Farthing CA & Xi L (2015) Inosine and hypoxanthine as novel biomarkers for cardiac ischemia: from bench to point-of-care. *Exp Biol Med Maywood NJ* **240**, 821–831.
200 T D, Td N & Ed A (2013) Cardiac metabolism in heart failure: implications beyond ATP production. *Circ Res* **113**, 709–724.
201 Heerlein K, Schulze A, Hotz L, Bärtsch P & Mairbäurl H (2005) Hypoxia decreases cellular ATP demand and inhibits mitochondrial respiration of a549 cells. *Am J Respir Cell Mol Biol* **32**, 44–51.
202 Oláh J, Klivényi P, Gardián G, Vécsei L, Orosz F, Kovacs GG, Westerhoff HV & Ovádi J (2008) Increased glucose metabolism and ATP level in brain tissue of Huntington's disease transgenic mice. *FEBS J* **275**, 4740–4755.
203 Ebanks B, Ingram TL & Chakrabarti L (2020) ATP synthase and Alzheimer's disease: putting a spin on the mitochondrial hypothesis. *Aging* **12**, 16647–16662.
204 Zhang C, Rissman RA & Feng J (2015) Characterization of ATP Alternations in an Alzheimer's Transgenic Mouse Model. *J Alzheimers Dis JAD* **44**, 375–378.
205 Nakano M, Imamura H, Sasaoka N, Yamamoto M, Uemura N, Shudo T, Fuchigami T, Takahashi R & Kakizuka A (2017) ATP Maintenance via Two Types of ATP Regulators Mitigates Pathological Phenotypes in Mouse Models of Parkinson's Disease. *EBioMedicine* **22**, 225–241.
206 Chen R, Park H-A, Mnatsakanyan N, Niu Y, Licznerski P, Wu J, Miranda P, Graham M, Tang J, Boon AJW, Cossu G, Mandemakers W, Bonifati V, Smith PJS, Alavian KN & Jonas EA (2019) Parkinson's disease protein DJ-1 regulates ATP synthase protein components to increase neuronal process outgrowth. *Cell Death Dis* **10**, 1–12.
207 Deli T & Csernoch L (2008) Extracellular ATP and cancer: an overview with special reference to P2 purinergic receptors. *Pathol Oncol Res POR* **14**, 219–231.
208 Seyfried TN, Arismendi-Morillo G, Mukherjee P & Chinopoulos C (2020) On the Origin of ATP Synthesis in Cancer. *iScience* **23**, 101761.

209 Wallace DC (2012) Mitochondria and cancer. *Nat Rev Cancer* **12**, 685–698.
210 Di Virgilio F, Sarti AC, Falzoni S, De Marchi E & Adinolfi E (2018) Extracellular ATP and P2 purinergic signalling in the tumour microenvironment. *Nat Rev Cancer* **18**, 601–618.
211 Qian Y, Wang X, Li Y, Cao Y & Chen X (2016) Extracellular ATP a New Player in Cancer Metabolism: NSCLC Cells Internalize ATP In Vitro and In Vivo Using Multiple Endocytic Mechanisms. *Mol Cancer Res MCR* **14**, 1087–1096.
212 McCafferty CE, Abi-Hanna D, Aghajani MJ, Micali GT, Lockart I, Vickery K, Gosbell IB & Jensen SO (2018) The validity of adenosine triphosphate measurement in detecting endoscope contamination. *J Hosp Infect* **100**, e142–e145.
213 Sanna T, Dallolio L, Raggi A, Mazzetti M, Lorusso G, Zanni A, Farruggia P & Leoni E (2018) ATP bioluminescence assay for evaluating cleaning practices in operating theatres: applicability and limitations. *BMC Infect Dis* **18**, 583.
214 Nante N, Ceriale E, Messina G, Lenzi D & Manzi P (2017) Effectiveness of ATP bioluminescence to assess hospital cleaning: a review. *J Prev Med Hyg* **58**, E177–E183.
215 Watanabe A, Tamaki N, Yokota K, Matsuyama M & Kokeguchi S (2018) Use of ATP bioluminescence to survey the spread of aerosol and splatter during dental treatments. *J Hosp Infect* **99**, 303–305.
216 Okanojo M, Miyashita N, Tazaki A, Tada H, Hamazoto F, Hisamatsu M & Noda H (2017) Attomol-level ATP bioluminometer for detecting single bacterium. *Lumin J Biol Chem Lumin* **32**, 751–756.
217 Wallace KB (2008) Mitochondrial off targets of drug therapy. *Trends Pharmacol Sci* **29**, 361–366.

Table 1. Comparison of genetically-encoded ATP biosensors

Biosensor	Application	Fluorophores (λex/λem; nm) or reporters	Validation done in:	Optimization/Biological application	K_D
ATEAM [138]	FRET	mseCFP (435/475); cp173-mVenus (515/527)	HeLa		3.3 mM
GO-ATEAM [149]	FRET	cp173-mEGFP (470/510); mKOκ (551/560)	HeLa	*Optimization of the original ATEAM sensor:* less phototoxic excitation wavelength for prolonged observations	7.1 mM
ATEAM1.03NL [141]	FRET	mseCFP (435/475); cp173-mVenus (515/527)	*Drosophila melanogaster; Caenorhabditis elegans*	*Optimization of the original ATEAM sensor:* monitoring of intracellular ATP at 25°C	1.8 mM
EAF-ATP [151]	FRET [138,141,147,149–151]	GFP (488/507); YFP (513/527)	U87 and U87vIII	*Optimization of the original ATEAM sensor:* emission of an enhanced fluorescent signal	not specified

ecATEAM3.10 [147]	FRET	CFP (456/480); YFP (513/527)	N2A, HEK293 and SK-MEL-5	*Optimization of the original ATEAM sensor:* Monitoring of extracellular ATP	12 µM
Syn-ATP [155]	Bioluminescence	mCherry (587/610); Luciferase	Hippocampal neurons	*Monitoring of synaptic activity*	2 mM
BTEAM [159]	BRET	NanoLuciferase; Venus (λem 528)	HeLa, Cos7, HepG2, HEK293A, PC12, B16F10	*Optimization of the original ATEAM sensor:* does not require the use of a laser as excitation source	0 to 10 mM
Nano-lantern [160]	BRET and CSL	Split-NanoLuciferase; Venus (λem 528)	living animals and plants	*Optimization of the original ATEAM sensor:* Usable for high-throughput drug screening and single-cell tracking	0.3 mM
ARSeNL [161]	BRET	NanoLuciferase; mScarlet (λem=594)	HEK293A and mice	*Optimization of the original BTEAM sensor*	1.1 mM
QUEEN [169]	Ratiometric	circularly-permutated enhanced GFP (400-494/513)	Bacterial cells	*Optimization of the original ATEAM sensor:* monitoring of ATP compatible with bacterial growth rate	QUEEN-7µ 7 µM QUEEN-2m 2 mM
iATPSnFR [170]	Intensiometric	circularly-permutated superfolder GFP (488/525)	HEK293 and U373	*Monitoring of ATP in the extracellular space*	3 mM
MaLion (R, G and B) [171]	Intensiometric	Red (565/585) Green (505/522) Blue (373/446)	HeLa, primary adipocytes and *C. elegans*	*low pH sensitivity*	MaLionG: 1.1 mM MaLionR: 0.34 mM MaLionB: not specified
Perceval [172]	Ratiometric	circularly permuted Venus (405-490/530)	Mammalian cells and yeast	*Monitoring of the ADP/ATP ratio*	0.3 mM

Table 2. Comparison of the different techniques available for ATP monitoring

Techniques for monitoring ATP	Type of samples	Readout	Spatiotemporal resolution	Equipment	Detection time	Sensitivity
NMR [94–96]	Cell extracts serum, plasma	Quantitative	No	NMR spectrometer	≈ 14 h	**mM**
HPLC [103–106]	Cell extracts serum, plasma	Quantitative	No	Chromatograph	≈ 20 min	**pmol**
LC-MS/MS [108,109]	Cell extracts serum, plasma	Quantitative	No	Mass spectrometer	< 10 min	**nmol**
Respirometry [110]	Intact cells, mitochondrial fractions	Qualitative	No	Oxygraph	≈ 90 min	**%**
Electrochemiluminescent Sensors [123]	Serum	Quantitative/ Qualitative	No	Spectrometer, electrodes	≈ 5 min	**nmol**
Chemoluminescent Sensors [122,129]	Intact cells	Quantitative/ Qualitative	Yes	Spectrometer or confocal microscope	≈ 15 sec	**mM**
Bioluminescent Sensors [146,153,154]	Cell extracts, plasma, mitochondrial fractions	Quantitative/ Qualitative	No	Spectrometer or luminometer	< 5 min	**pmol**
BRET sensors [159–161]	Intact cells	Quantitative/ Qualitative	Yes	Spectrometer, luminometer or fluorescence microscope	< 20 min	**mM**
Single-wavelength sensors [169–171,175]	Intact cells	Quantitative/ Qualitative	Yes	Spectrometer or fluorescence microscope	< 1 min	**µM**

FRET sensors [138,141,147,149–151]	Intact cells	Quantitative/ Qualitative	Yes	Spectrometer or fluorescence microscope	< 1 min	**µM**

Figure legends

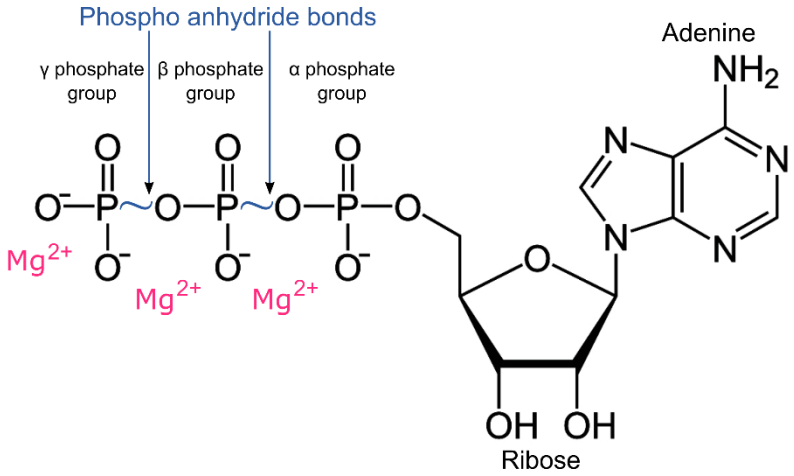

Figure 1. Chemical representation of ATP. ATP is a nucleotide composed of adenine (purine base), ribose (pentose) and of 3 phosphate groups. Within the cell, ATP is stabilized by Mg^{2+} in order to form a Mg^{2+}-ATP complex.

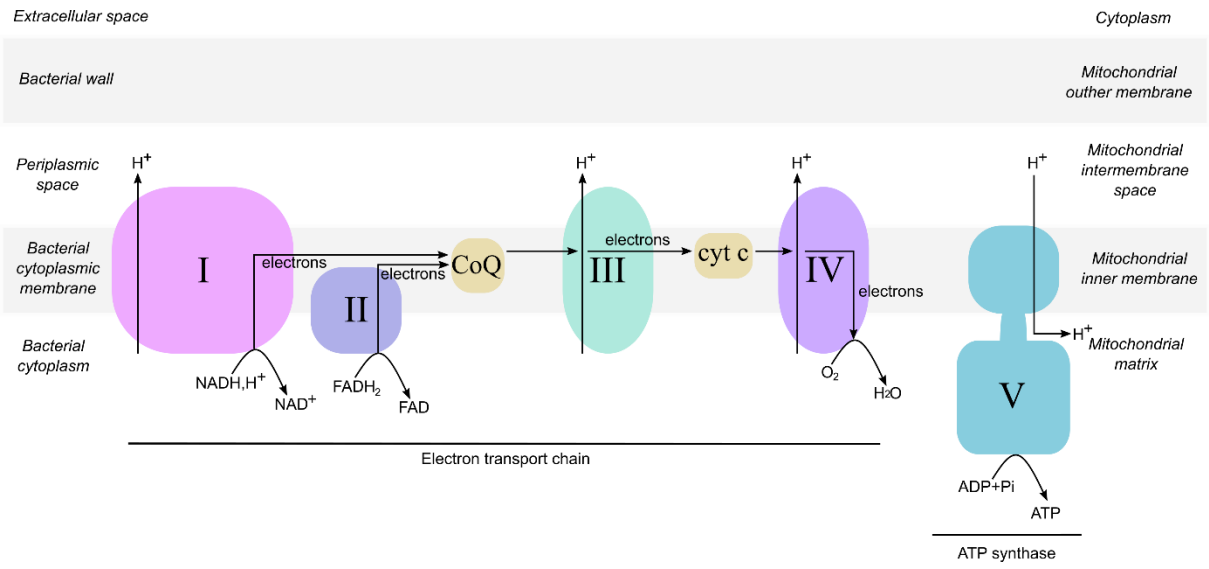

Figure 2. Schematic representation of the respiratory chain. In bacteria, the respiratory chain is located in the cytoplasmic membrane (left panel, italics) and in the inner mitochondrial

membrane in eukaryotes (right panel, italics). It is composed of an electron transport chain that creates a proton gradient in the periplasmic space for bacteria, and in the mitochondrial intermembrane space for eukaryotes. Then, the proton gradient is translocated through the ATP synthase to the periplasmic space in bacteria, or to the mitochondrial matrix in eukaryotic cells. This translocation allows the rotation of the ATP synthase at the structural level, and ATP will be converted from an ADP + inorganic phosphate (P_i) reaction.

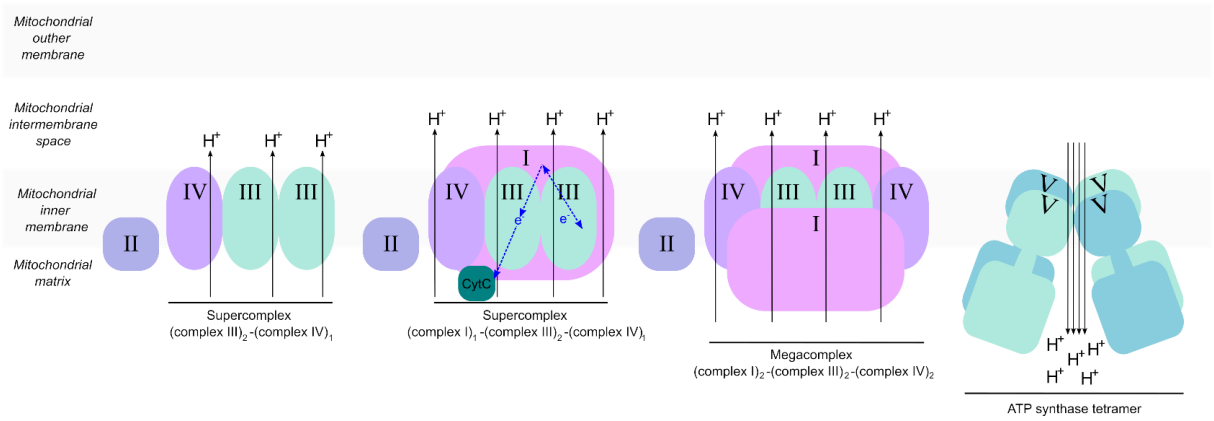

Figure 3. Organization of electron transport chain and ATP synthase inside mitochondria. A megacomplex, [(complex I)$_2$-(complex III)$_2$-(complex IV)$_2$] is the result of the association of supercomplexes (or respirasomes) [(complex III)$_2$-(complex IV)$_1$] or [(complex I)$_1$-(complex III)$_2$-(complex IV)$_1$]. ATP synthase (complex V) has the ability to form dimers or tetramers inside mitochondria. Dashed lines: representative view of the "bifurcated" electron flow within the supercomplex. One electron is transferred to cytochrome c, the other is recycled back to complex I [51,52].

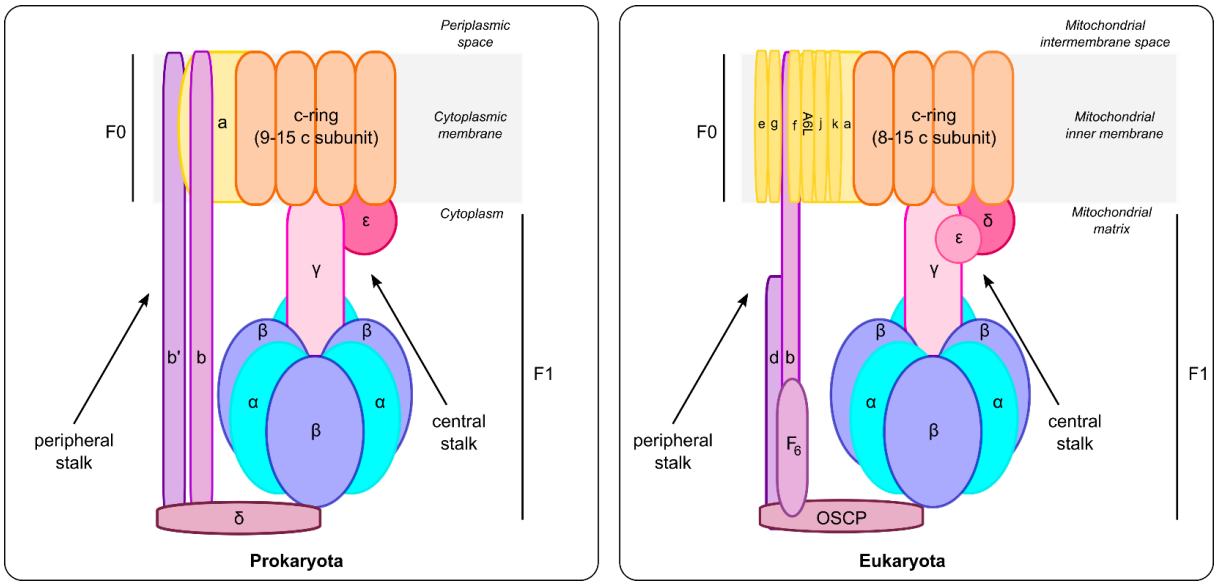

Figure 4. Structural comparison of the bacterial and mitochondrial ATP synthase machineries. *Left panel:* the bacterial ATP synthase consists of a rotor part F0 (yellow, orange), forming the proton channel by subunit a and $c_{9\text{-}15}$. F0 also carries a central stalk (pink), composed by the γ and ε subunits. The static part F1 is formed by the peripheral stalk (purple) and the catalytic headpiece (blue). The peripheral stalk is constituted by the b, b' and δ subunits, and the catalytic headpiece by the α_3-β_3 subunits (blue). *Right panel:* Mitochondrial ATP synthase consists of rotor part F0 (yellow, orange), forming the proton channel by subunit a and $c_{8\text{-}15}$, in addition to subunits e, g, f, A6L, j and k. As in bacteria, F0 also carries a central stalk (pink) composed by the γ, δ and ε subunits. The F1 is formed by the peripheral stalk (purple) and the catalytic headpiece (blue). The peripheral stalk is composed of the b, d, F6 and OSCP subunits, and the catalytic headpiece is constituted by the α_3-β_3 subunits (blue). *Note:* The mitochondrial subunit δ corresponds to the bacterial subunit ε, whereas the mitochondrial ε subunit does not exist in bacteria.

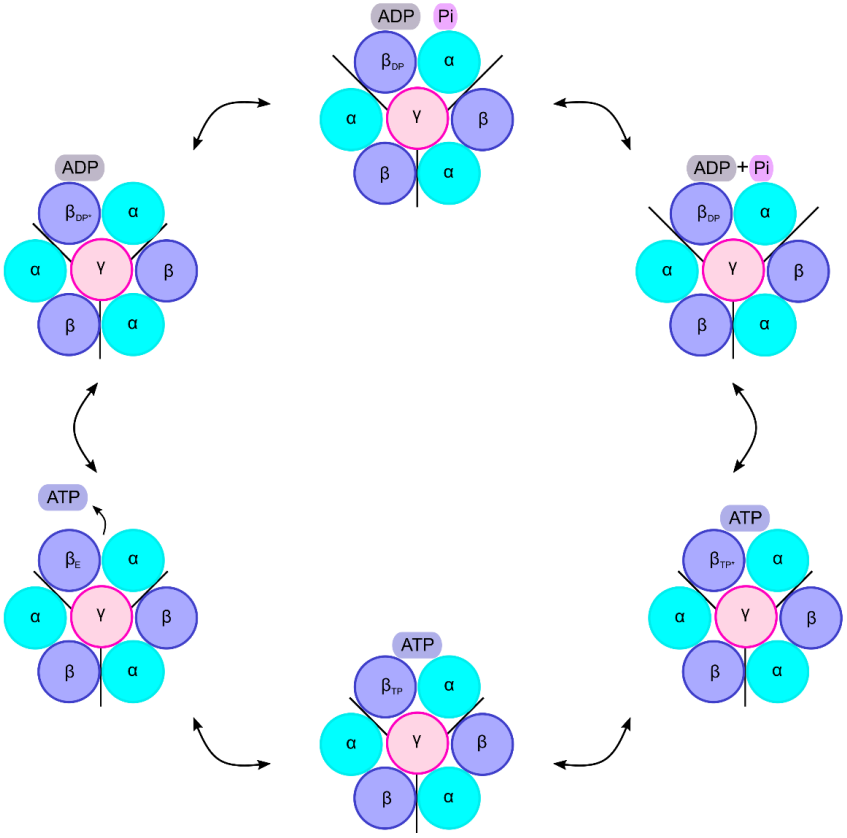

Figure 5. Rotational catalysis is the mechanism of ATP production by the ATP synthase. Each of the β subunits of the ATP synthase are found in a loose, tight or open conformation allowing the synthesis and the release of ATP molecules. The loose conformation (β_{DP}), corresponds to the binding of ADP and P_i. The tight conformation (β_{TP}), corresponds to the formation of a bond between the ADP and P_i. The open conformation (β_{E}), corresponds to the release of the newly-formed ATP molecule into the mitochondrial matrix (or bacterial cytoplasm).

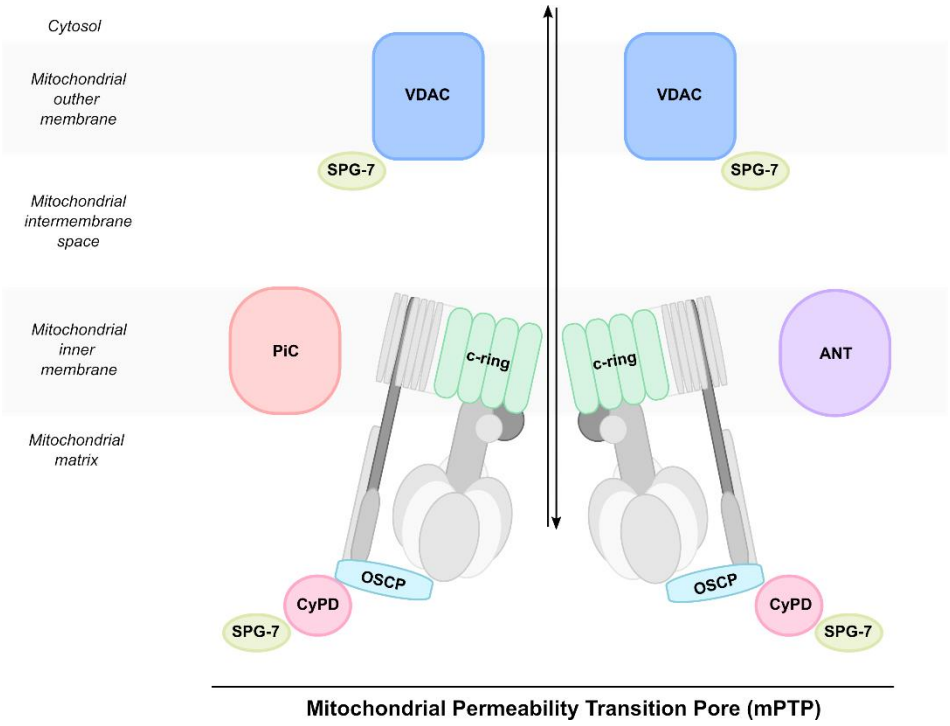

Figure 6. Composition of the mPTP. ATP synthase can arrange in dimers and associate with partners such as cyclophilin D (CyPD), adenine nucleotide translocase (ANT), the outer membrane voltage-dependent anion channel (VDAC), the phosphate carrier (PiC) and spastic paraplegia 7 (SPG-7) to form the mitochondrial Permeability Transition Pore (mPTP).

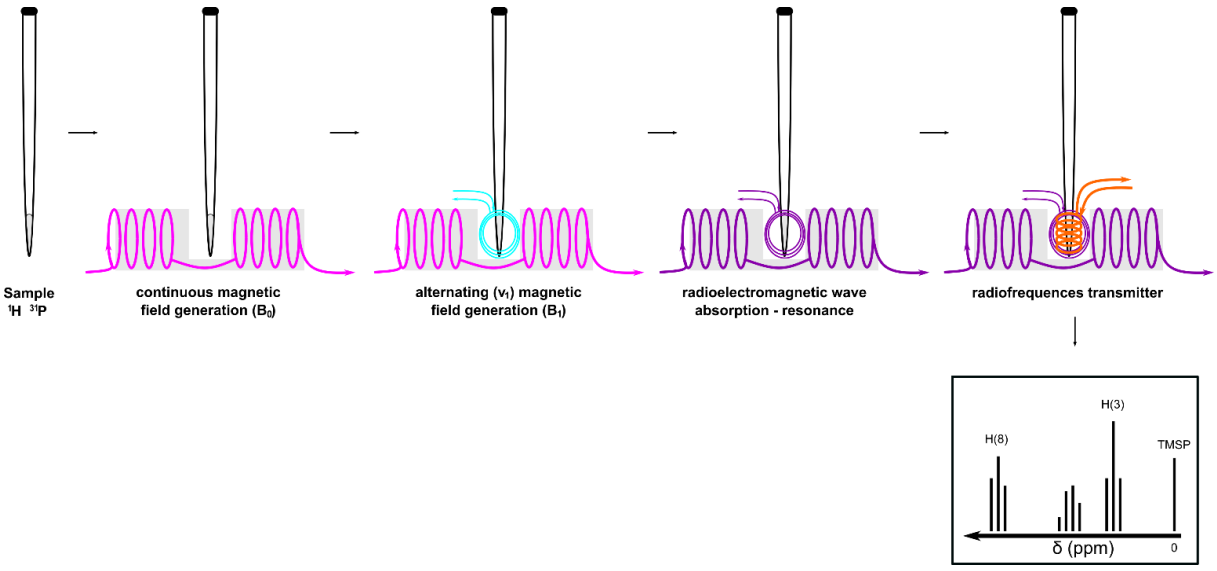

Figure 7. Principle of Nuclear Magnetic Resonance. The spectrometer consists of a magnet and several coil systems. The sample is placed in a superconducting magnet (or

electromagnet), in which a continuous magnetic current (magenta) is generated, creating a B_0 magnetic field of up to 25 Tesla [99]. Then, a radiofrequency oscillator generates an alternating magnetic current (cyan) B_1 at the frequency v_1, called resonance frequency, of 60 to 950 MHz [100,101]. A radio-electromagnetic wave is thus generated (purple). The analysed atom absorbs this radio-electromagnetic wave, and is capable to resonate. It will then emit energy peaks that can be captured on an NMR spectrum thanks to a radiofrequences transmitter (orange), which detects and recovers the radiofrequencies, and transmits them to a computer. On this spectrum, the reference (peak at 0 ppm on the x-axis) corresponds to the internal standard, which is a molecule with a known resonance frequency and that can be used as a reference. This reference compound (TMSP) has very low toxicity, an overall chemical inertia and emits a single peak on the spectrum. Since ATP, ADP and AMP molecules contain a significant proportion of H and P atoms, their relative signals on the NMR spectrometer will differ from the one of TMSP.

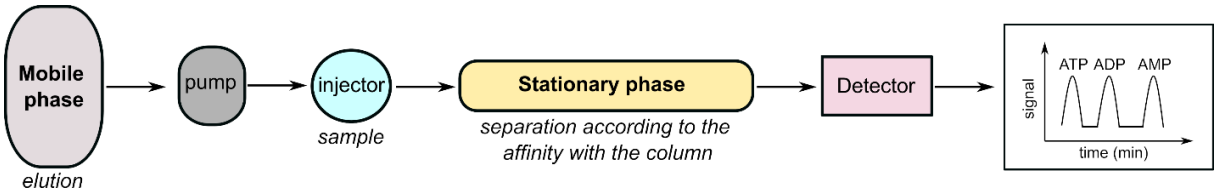

Figure 8. Principle of High-Performance Liquid Chromatography. The mobile phase, constituted by solvents with different polarity properties, will pass through a pump which will put the mobile phase under pressure. Then, the injector will put the samples in contact with the mobile phase, which then passes through the stationary phase. The stationary phase is a column that will separate the different molecules of the sample according to their affinity the solvents. At the exit of the column, the detector will detect the molecules of interest using either UV/visible radiations, fluorescence emission, or a mass spectrometry system. The information will then be processed by a computer, which will then generate a chromatogram as an output.

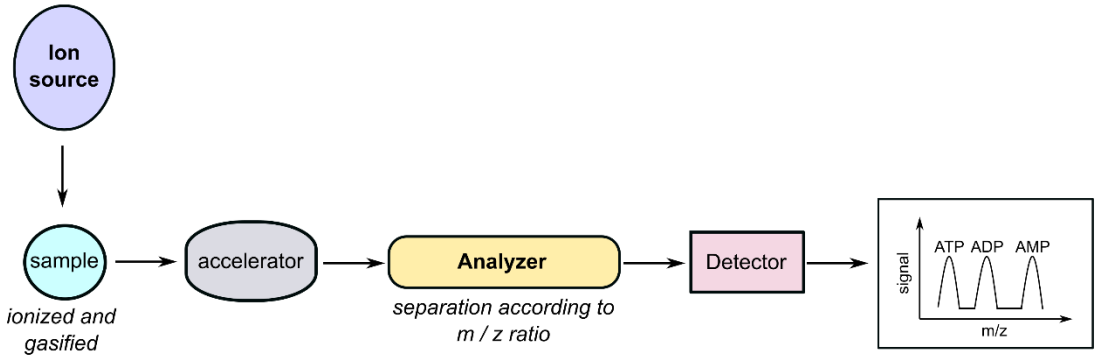

Figure 9. Principle of Mass Spectrometry for ATP quantification. First, the sample is prepared by integrating it into a matrix and placed inside a spectrometer. The ion source (nitrogen laser) irradiates the sample and genererates heating, which converts the sample from a solid state to a gaseous state. Then, this irradiation causes collision events between the molecules of the sample and the matrix. These events will trigger the transfer of protons from the matrix to the sample, thus leading to ionization. The sample passes through an acceleration zone which is negatively charged, and the molecules of the sample therefore a certain speed, which is inversely proportional to the mass (m) or charge (z) of the molecule. Then, the molecules enter the analyzer which will separate the molecules according to their m/z ratio. At the exit of the analyzer, the molecules of interest will be detected and processed by a computer to generate a spectrum.

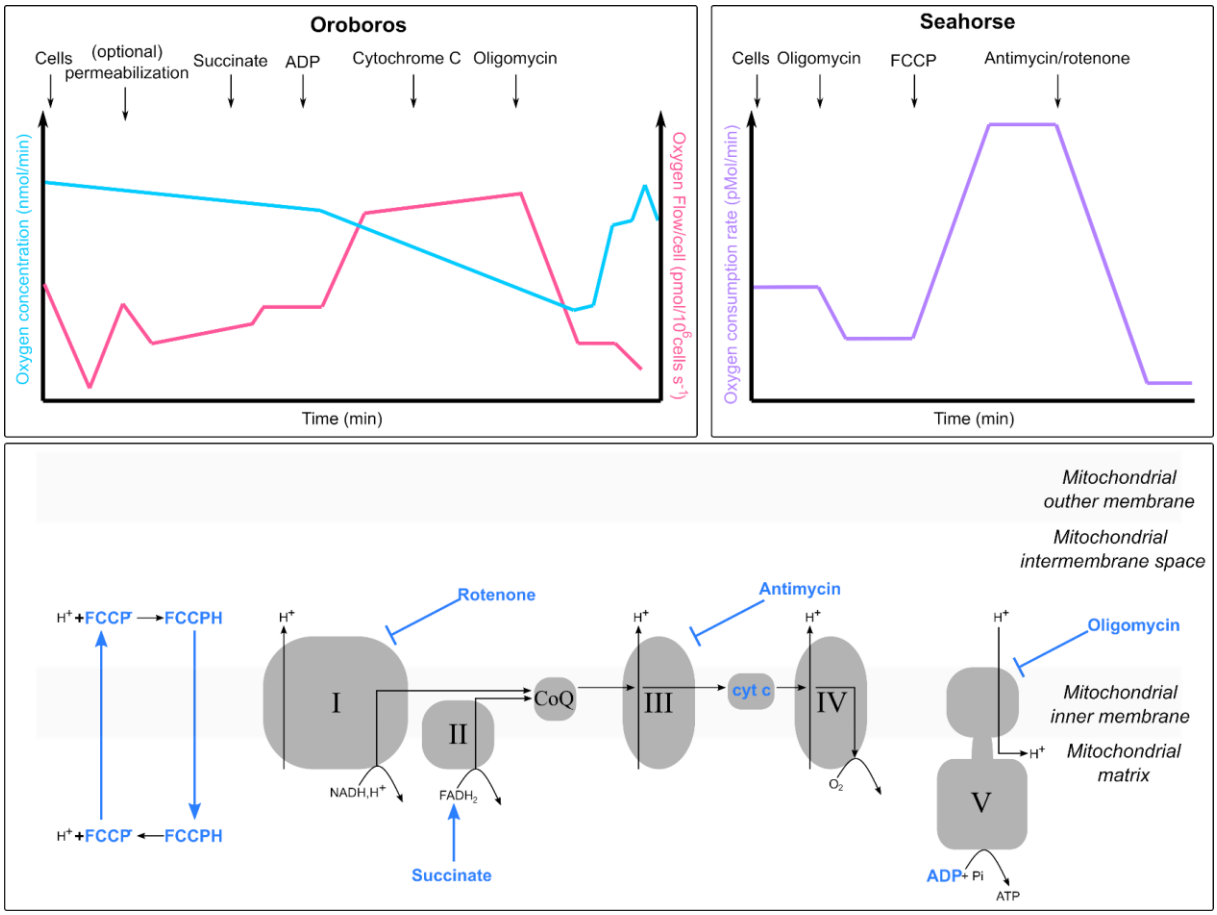

Figure 10. Respirometry: principle, chemicals used and expected output. *(Top panels)* Oroboros (left) *versus* Seahorse-type (right) traces. Both approaches allow to determine oxygen consumption, which varies in function of the drugs and/or the metabolites injected. *(Bottom panel)* Representation of the mechanisms of actions of the drugs / metabolites used in respirometry. FCCP inhibits ATP production by inhibiting proton reflux through the ATP synthase. By associating with complex III, antimycin inhibits ATP production by inhibiting the formation of the proton gradient. By associating with complex I, rotenone inhibits ATP production by inhibiting proton gradient formation. Oligomycin inhibits ATP production by blocking proton influx through the ATP synthase. Succinate, cytochrome c and ADP are the most relevant metabolites used in respirometry experiments.

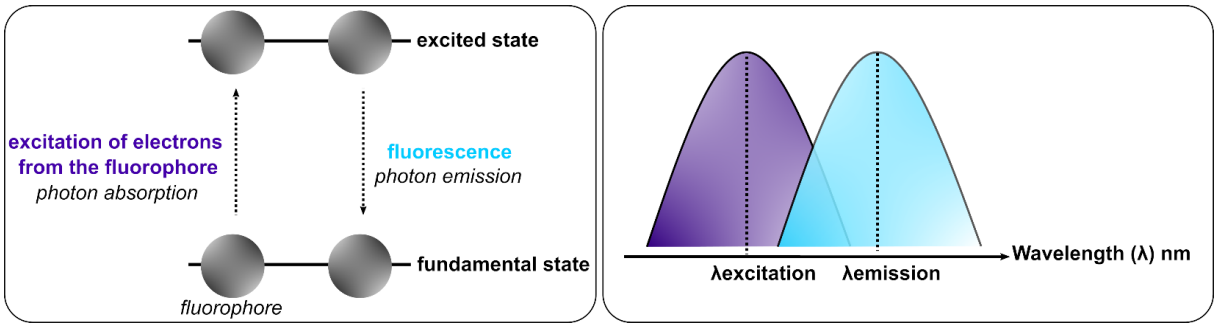

Figure 11. Principle of fluorescence and excitation/emission spectra of fluorophores. Fluorescence is the phenomenon of photon emission by a fluorophore. *Left panel*: a fluorophore is excited, it absorbs photons and changes from a stable (or fundamental) state to an unstable (or excited) state. To return to the fundamental state, the fluorophore emits photons at a given wavelength, resulting in fluorescence emission. *Right panel*: each fluorophore is excitable and emits at a particular wavelength (λexcitation/λemission, respectively). This constitutes the excitation/emission spectra of the fluorophore.

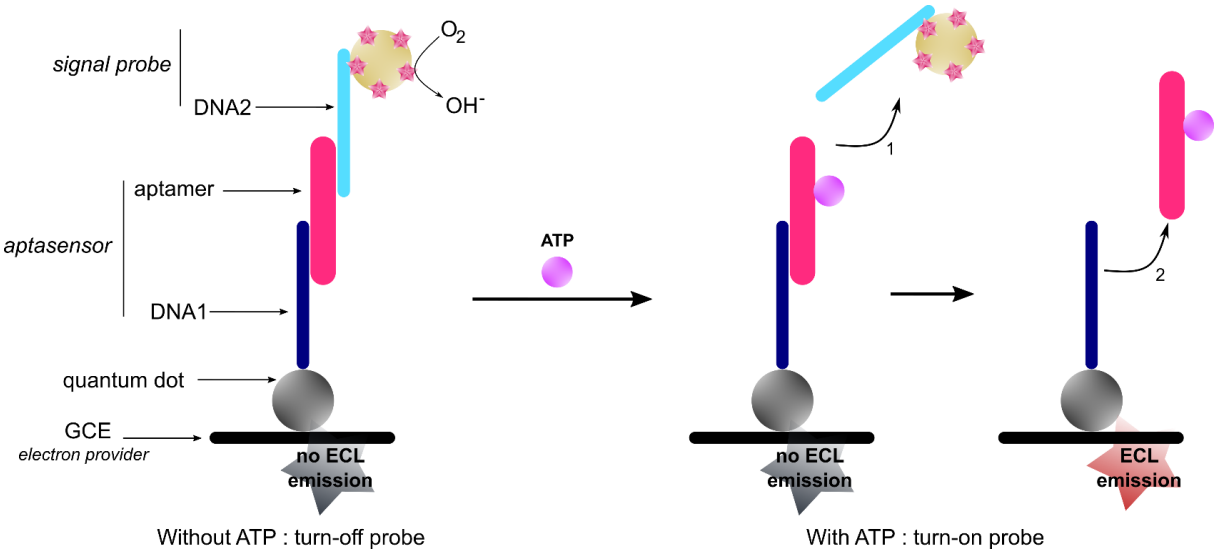

Figure 12. Functioning mode of an electrochemiluminescence-based ATP probe. This type of luminescence is initiated by an electron transfer. The quantum dot is fixed to an electrode (GCE) and then linked to the aptasensor. The aptasensor consists of a DNA sequence (DNA1) and a synthetic oligonucleotide (aptamer) capable of binding ATP. The DNA1 is partially complementary with the aptamer, a synthetic oligonucleotide capable of binding a specific

ligand such as ATP, and the signal probe. The signal probe is a DNAzyme, which consists of a second DNA sequence (DNA2, also partially complementary with the aptamer) and a gold nanoparticle associated with a hemin molecule. *Left panel:* if there is no ATP, the aptasensor is linked to the signal probe, which is able to reduce O_2 into OH^- and leading to a drastic decrease in the emission of ECL. *Right panel:* if ATP is present, the aptamer will preferentially bind it. This will detach the signal probe from the aptamer, and it will allow a significant ECL emission.

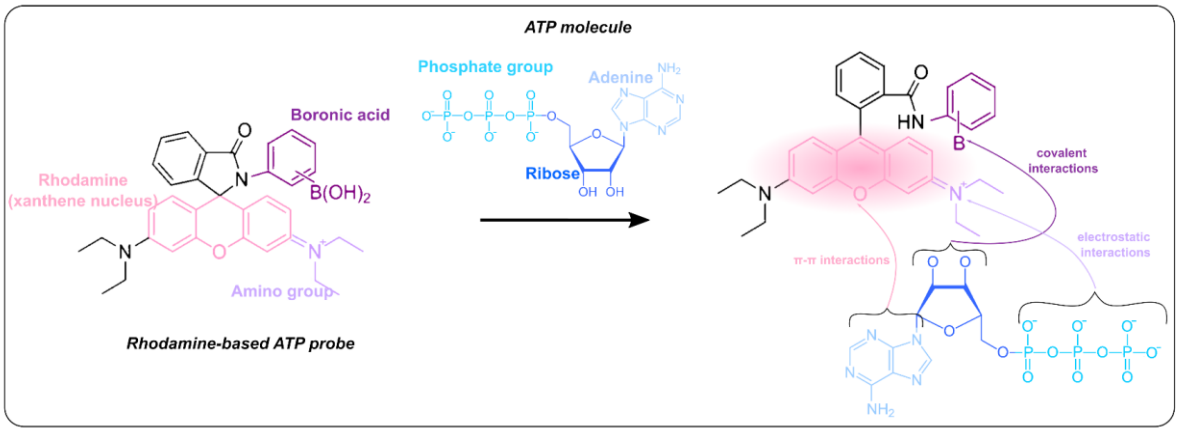

Figure 13. Molecular representation of the rhodamine-based ATP probe. In the absence of ATP, the probe has a closed ring structure and no chemiluminescence is detectable. In the presence of ATP, three specific interactions take place: 1- covalent interactions between the rhodamine molecule and the ribose group; 2- π-π interactions between the xanthene nucleus of rhodamine and adenine; 3- electrostatic interactions between the amino groups of the rhodamine molecule and the phosphate group of ATP. These interactions open the ring and allow rhodamine light emission [131].

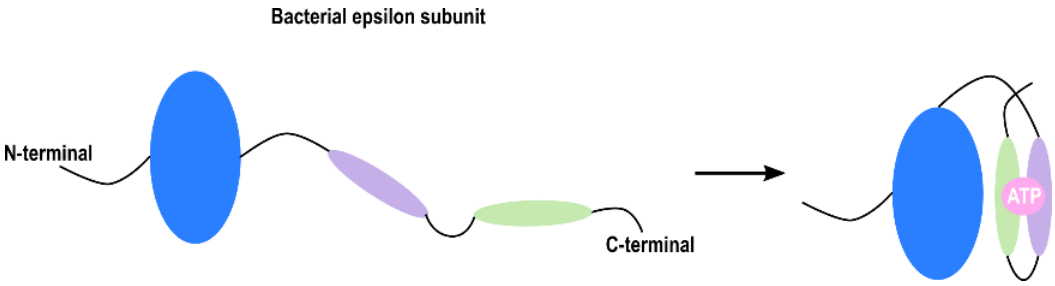

Figure 14. Principle of the ε bacterial ATP synthase subunit. This protein is composed of a β-barrel domain located at the N-terminus (blue), and a α-helical domain with 2 helices (purple and green) located at the C-terminus. Upon ATP binding (in pink), the two α-helices interact and lead to a three-dimensional conformational change of the ε subunit. Overall, this subunit can adopt 2 different conformations: open (ATP-free) or close (ATP-bound) [138,141]. The ribbon diagram corresponding to the structure of the biosensor can be found in Yoshida et al, [142].

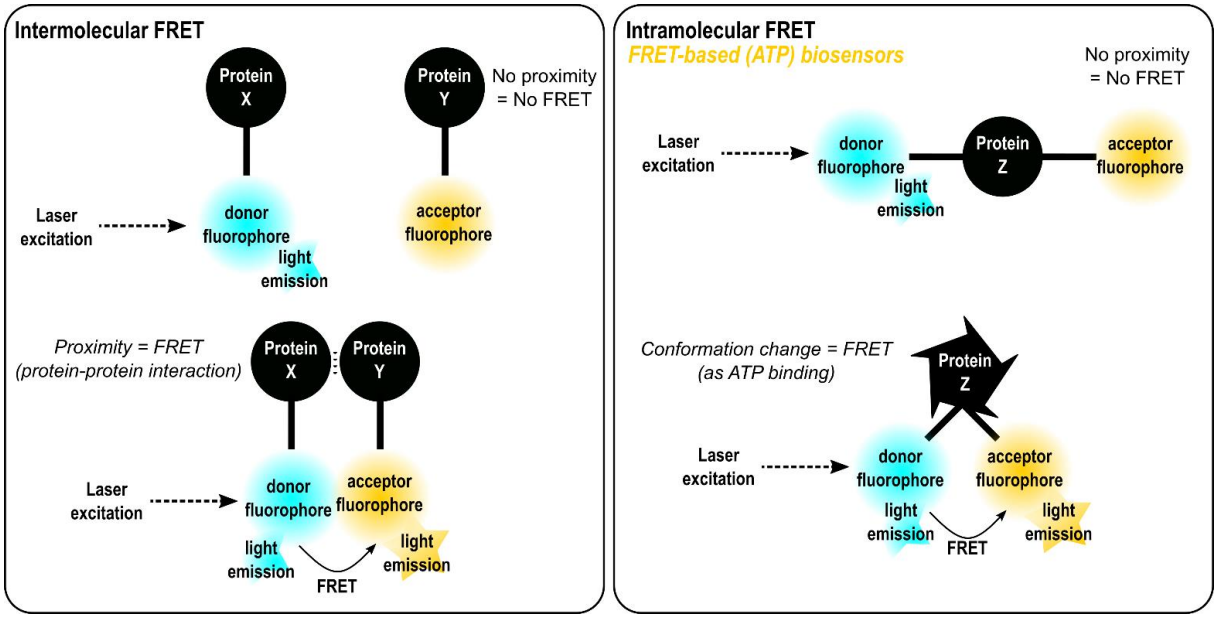

Figure 15. Principle of Fluorescence Resonance Energy Transfer and FRET-based biosensors. When the donor and acceptor fluorophores are close (≤10 nm), the energy derived from the excitation of the donor is partially transferred to the acceptor fluorophore, which can emit light without direct excitation. *Left panel:* a first protein (X) is fused with a donor fluorophore,

and a second protein (Y) with an acceptor flurorophore. If the proteins do not interact, the FRET phenomenon cannot occur and the acceptor fluorophore cannot emit light. Conversely, FRET can occur if the proteins interact, which leads to fluorescence emission from the acceptor. *Right panel:* a protein (Z) is inserted within a donor/acceptor pair. The FRET phenomenon occurs if the protein adopts a specific 3D conformation bringing the donor/acceptor pair in proximity. This property is used to develop FRET-based biosensors.

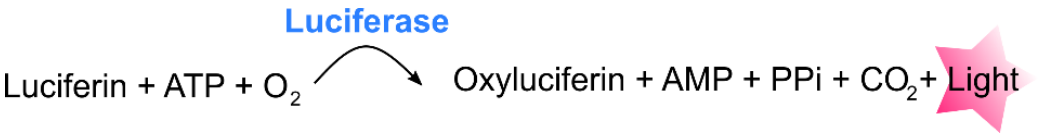

Figure 16. Principle of the luciferase reaction in luciferase-based ATP assays. In presence of luciferin, oxygen and ATP, the luciferase generates oxyluciferin, AMP, pyrophosphate anion, CO_2 and photons emission (light).

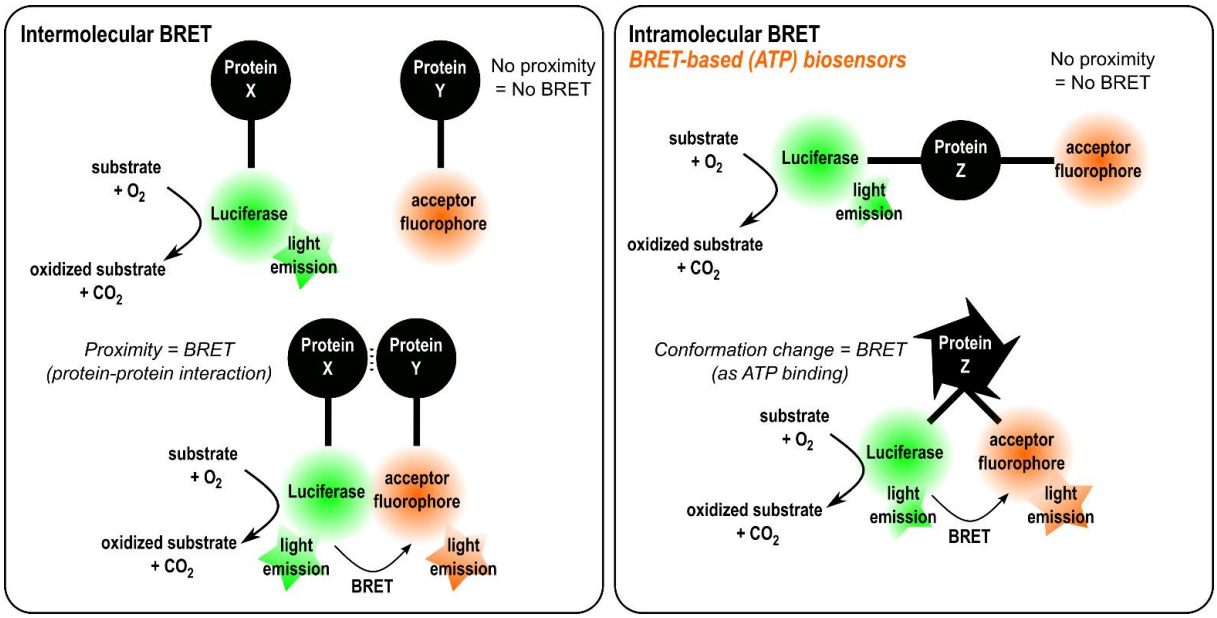

Figure 17. Principle of Bioluminescence Resonance Energy Transfer and BRET-based biosensors. When a luciferase and a fluorophore are close (≤10 nm), the energy derived from a luciferase reaction excites the fluorophore. The fluorophore can, in turn, emit light. *Left panel:* a putative protein (X) is fused to a luciferase and a second putative protein (Y) is fused

to a flurorophore. If X and Y proteins do not interact, the BRET phenomenon cannot occur, and the fluorophore will not emit light. Conversely, the interaction of X and Y allows the BRET phenomenon to occur, and as a consequence, the fluorophore will emit light. *Right panel:* a putative protein Z is fused with a luciferase and a flurorophore at each terminus. Conformational folding events allow the BRET phenomenon to occur, and this property is used to develop BRET-based biosensors.

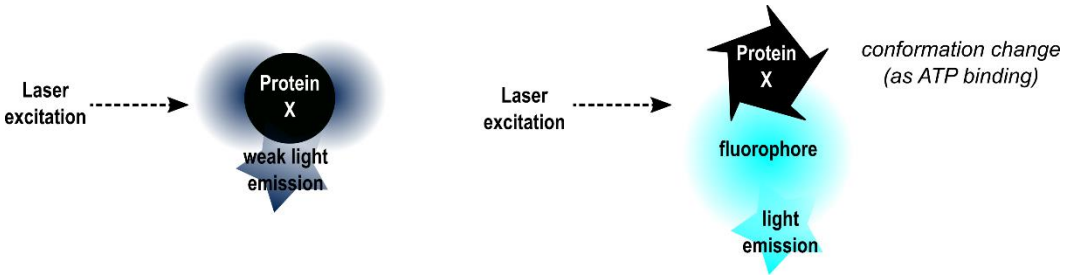

Figure 18. Single-fluorophore ratiometric and intensiometric biosensors. A putative protein (X) is fused to a circularly-permutated fluorophore. If the target protein undergoes a conformational change, the fluorophore is capable to exhibit an increase in fluorescence emission.